Explosive Homogeneous Nucleation Boiling in Ethanol

by

Ashik Hasan

A Thesis Submitted in Partial Fulfillment of the Requirements for the Degree of
MASTER OF SCIENCE IN MECHANICAL ENGINEERING

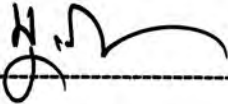**Department of Mechanical Engineering**
BANGLADESHUNIVERSITY OF ENGINEERING AND TECHNOLOGY
Dhaka-1000, Bangladesh

January 2016

The thesis titled "**Explosive Homogeneous Nucleation Boiling in Ethanol**," submitted by **Ashik Hasan,** Student no: 0412102015 P, Session: April, 2012 has been accepted as satisfactory in partial fulfillment of the requirement for the degree of MASTER OF SCIENCE IN MECHANICAL ENGINEERING on February 20, 2016.

BOARD OF EXAMINERS

1. ---   Chairman

Dr. Mohammad Nasim Hasan
Associate Professor
Department of Mechanical Engineering
BangladeshUniversity of Engineering and Technology (BUET)
Dhaka-1000, Bangladesh.

2. ---   Member

Head   (Ex-officio)
Department of Mechanical Engineering
BangladeshUniversity of Engineering and Technology (BUET)
Dhaka-1000, Bangladesh.

3. ---   Member

Dr. A.K.M. Monjur Morshed
Assistant Professor
Department of Mechanical Engineering
BangladeshUniversity of Engineering and Technology (BUET)
Dhaka-1000, Bangladesh.

4. ---   External

Dr. Md. Abdur Razzaq Akhanda
Ex-Professor
Department of Mechanical Engineering
Bangladesh University of Engineering and Technology (BUET)
Dhaka-1000, Bangladesh.

CANDIDATE'S DECLARATION

It is hereby declared that this thesis or any part of it has not been submitted elsewhere for any degree or diploma.
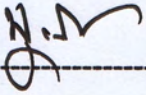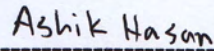
Ashik Hasan

Ashik Hasan

CERTIFICATE OF RESEARCH

This is to certify that the work presented in this thesis is carried out by the author under the supervision of Dr. Mohammad Nasim Hasan, Associate Professor of Department of Mechanical Engineering, Bangladesh University of Engineering & Technology, Dhaka.

Dr. Mohammad Nasim Hasan

Ashik Hasan

Dedicated to My Family

ACKNOWLEDGEMENT

I am very grateful to my supervisor, Dr. Mohammad Nasim Hasan, for all the time and efforts he has put in towards guiding my dissertation work. I am indebted to him for giving me invaluable support, for showing incredible patience with me and encouraging me at every step of this dissertation, which would not have been possible without guidance and help of him. His dedication and hard work towards the research will be a constant source of inspiration for me.

I would like to thank the members of my thesis evaluation committee, Dr. Md. Abdur Razzaq Akhanda, Dr. Md. Zahurul Haq and Dr. A.K.M. Monjur Morshed for their valuable comments and suggestions.

 I want to especially thank my late father who has always inspired and motivated me and always believed in me even when I did not believe in myself. I thank my mother for her unwavering support towards me throughout my academic life.

I want to also thank my friends who have helped me during this dissertation work. Without their help in collecting various literatures and article, writing and editing the thesis, this work would not have been possible.

ABSTRACT

The characteristics of homogeneous boiling in ethanol subjected to rapid heating with a linearly increasing boundary temperature condition have been studied by applying a macroscopic model based on analytical solution of 1-D semi-infinite heat conduction in association with molecular theory of homogeneous nucleation boiling. In this model, a finite control volume or cluster at the liquid boundary is considered where energy is stored due to external heating while some energy is consumed because of bubble nucleation and subsequent growth. The corresponding energy balance equation in the liquid cluster is obtained by considering these two competing parallel processes. A particular state has been defined as the boiling explosion condition when massive scale vaporization causes the liquid sensible energy to decrease i.e. the instantaneous rate of boiling heat consumption at a moment exceeds the external energy deposition within the liquid cluster. Two different length scales for the size of liquid cluster has been adopted- (i) size of a critical vapor embryo and (ii) thermal penetration depth. For ethanol heating with initial and boundary conditions identical to those reported in the literature, the present study shows that the model can predict the timing of the boiling explosion condition with reasonable agreement if the size of liquid cluster is considered to be that of a critical vapor embryo at maximum liquid superheat. Then for different boundary heating rates, boiling explosion time and temperature for ethanol are obtained. The obtained times of boiling explosion vary almost in inverse order of heating rate, while boiling explosion temperatures vary about 9^0C over the entire range of heating rates. These results have been compared with the theoretical explosion condition obtained from molecular dynamics and pseudo-atomic model study as reported in the literature. It has been found that, the time and temperature at which explosive boiling in ethanol occurs; vary with the degree of liquid subcooling. Therefore, these parameters are not sufficient to describe the explosive boiling phenomena as a unique state regardless of heating method and parameter. To find a unique criterion for explosive boiling, an energy approach is taken in this study. Using this approach, for a given initial temperature, it has been found that, for a given liquid initial temperature (25^0C), when cumulative energy density reaches 3.28×10^8 - 3.44×10^8 J / m^3 for ethanol, explosive boiling will occur irrespective of liquid boundary heating conditions. Therefore, a unique criterion is found in the form of cumulative energy density near the boundary for the occurrence of explosive boiling in the liquid.

NOMENCLATURE

A_{slv}	Hamaker Constant	
b	Boundary Heating Rate	K/s
c_p	Specific Heat	$J/kg.K$
E	Cumulative Energy Deposited in The Liquid	J/m^2
$\dot{E}^*$	Cumulative Energy Density in The Liquid	J/m^3
h_c	Thickness of Stable Liquid Layer	m
h_p	Critical Distance of Maximum Supersaturation	m
J	Nucleation Event Rate	$m^{-3}s^{-1}$
L	Latent Heat of Vaporization	J/kg
M	Molecular Weight	$Kg/kmol$
m	Relative Energy Density Factor	
P_0	Bulk Liquid Pressure	Pa
P_s	Saturation Pressure	Pa
q_c	Energy Consumption Rate in The Cluster	W/m^2
q_d	Energy Deposition Rate in The Cluster	W/m^2
$q_{max,max}$	Upper Limit of Evaporative Heat Flux	W/m^2
q^*_{l-v}	Heat Flux Across Liquid-Vapor Interface at The Boiling Explosion	W/m^2
q_w	Boundary Heat Flux	W/m^2
R	Universal Gas Constant	$J/kg.K$
$r(t,t')$	Bubble Radius at Time t, Generated at t'	m
r_c	Radius of Critical Vapor Embryo	m
T	Temperature	K
T_0	Liquid Initial Temperature	^0C
T_i	Solid-Liquid Interface Temperature	^0C
T_{avg}	Average Temperature in The Liquid Cluster	K
T^*_{avg}	Maximum Cluster Temperature	K
t	Time	s
t^*	Time of Boiling Explosion	s
x_e	Liquid Cluster SIze	m

Greek

α	Thermal Diffusivity	m^2/s
Γ	Vapor Generation Rate	$kg/m^3.s$
δ^*_{th}	Thermal Penetration Depth	m
η	Modified Fourier Number	$\frac{x}{\sqrt{4\alpha t}}$
λ	Thermal Conductivity	$W/m.K$
ρ	Density	kg/m^3
σ	Surface Tension	N/m

Subscript/Superscript

l	Liquid
s	Solid
v	Vapor
$*$	State of Boiling Explosion

TABLE OF CONTENTS

LIST OF FIGURES

LIST OF TABLES

CHAPTER: ONE

INTRODUCTION

1.1 Introduction

Boiling Explosion or Explosive Boiling or Impact Boiling is a phenomenon that has drawn significant amount of attention in recent times. Previously boiling explosion had been studied only to understand the fatal accidents caused by it in Nuclear Reactor, Liquefied Natural Gas (LNG), Metallurgy, Paper Industry and Cryogenics [1-5]. But the concept of using the dispersed mechanical energy from rapidly expanding micro bubbles during boiling explosion to drive various MEMS (Micro Electro Mechanical Systems) devices has opened a new horizon in the field of boiling heat transfer research. Since micro scale science and technology is progressing rapidly, the thermo-physical problems in micro scale boiling explosion have become easily noticeable. That is why micro scale boiling explosion has become one of the most interesting topics for researchers of boiling heat transfer.

In this chapter, a brief explanation of boiling explosion phenomenon and associated bubble nucleation and growth will be given. Apart from that, some of the applications of boiling explosion phenomenon will be described briefly.

1.2 Explosive Boiling

Boiling is a well-known liquid to vapor phase change process. It can transfer large amount of energy under a comparatively lower temperature difference. It occurs at solid-liquid interface when a liquid is brought into contact with a surface having temperature much higher than the saturation temperature of the liquid at the corresponding pressure. In classical thermodynamics, phase change processes are regarded as quasi equilibrium events occurring at certain conditions corresponding to a saturation state. But real phase change processes occurring in non-equilibrium conditions deviate from classical thermodynamics assumption. Such is the case when liquid is superheated above boiling point during vaporization. Then liquid enters a meta-stable state in which the temperature of liquid is higher than the saturation temperature at system pressure. The degree of superheat ranges from few tenths of a degree to several tens of degrees and it depends on following factors:

2

(a) The liquid

(b) Nature of liquid container

(c) Volume of liquid

(d) Purity of liquid

(e) Rate of parametric variation (such as, liquid heating rate or depressurization rate etc.)

For very quick parametric variation, no vapor contact can be considered and notably high degrees of superheat are achievable. In such cases, boiling is triggered by homogeneous nucleation of bubbles, which is promptly followed by a large scale boiling with an explosive force. This instantaneous abrupt phase change event is referred as Boiling Explosion, Explosive Boiling or Impact Boiling.
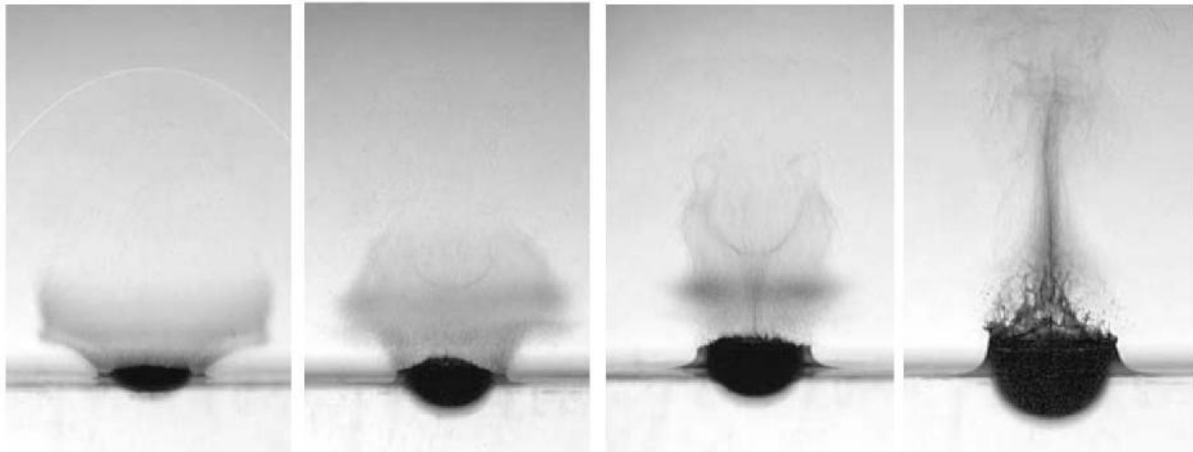
Fig. 1.1: Explosive Boiling or Boiling Explosion [6].

1.3 Bubble Nucleation

Bubble nucleation is a physical process in which a change of state occurs in a substance around certain focal point, known as nucleus. Once a nucleus is formed, it grows exponentially [7]. Therefore, before the formation of vapor in the bulk of liquid due to density fluctuation or at a solid surface with pre-existing gas or vapor pocket, a mechanically and thermally stable vapor bubble or nucleus must be formed [8]. Depending on the mechanism by which the nucleus is formed, bubble nucleation is divided into heterogeneous nucleation and homogeneous nucleation.

3

1.3.1 Heterogeneous Nucleation

In heterogeneous nucleation, foreign particles such as non-condensable gas or vapor bubble, dust particle etc. trapped in very narrow cracks and crevices in the heater surface provide the sites for vapor formation. It depends greatly on the properties and geometry of the heater surface. Vaporization during boiling occurs around these sites, so the nucleation is not uniform. Due to comparatively larger radius of these crevices, pre-existing bubbles require less energy to stabilize mechanically and thermally. Therefore, comparatively lower degree of superheat and pressure differential are generally found during heterogeneous nucleation [7, 8].

1.3.2 Homogeneous Nucleation

Homogeneous nucleation occurs when there are no impurities present which can act as a nucleus. It occurs spontaneously and uniformly in the substance. It depends mainly on liquid properties. Because of exceedingly quick parametric variation (pressure, temperature), a small but finite cluster of molecules acquires more energy than macroscopic average energy. With higher degree of superheat this group of molecules acquires more energy with increasing probability and forms a vapor nucleus. After the formation of vapor nucleus, bubble starts to form very rapidly and boiling occurs with explosive force [7, 8].

During any phase change process, the dominant mechanism is determined by the liquid properties, heated surface properties and the heating kinetics. Generally, at lower degree of superheat, heterogeneous nucleation is dominant and with the increase of degree of superheat, homogeneous boiling becomes more frequent.

1.4 Characteristics of Explosive Boiling

While superheating a certain volume of liquid by isobaric heating or adiabatic depressurization, energy is stored in liquid and some portion of this energy is consumed due to bubble nucleation and subsequent growth. Explosive boiling or boiling explosion occurs when the consumed energy by bubble nucleation becomes equal or exceeds the stored energy.

Temperature in the liquid increases until the occurrence of explosive boiling phenomenon and then decreases drastically, which is due the decrease of sensible energy. The maximum temperature is reached at the moment when consumed energy is equal to stored energy. For a certain heating rate, explosive boiling occurs around same temperature regardless of the size of liquid volume.

With increasing heating rates, time required for explosive boiling condition decreases and liquid penetrates deeper into the meta-stable state. Variation of time of explosive boiling occurs almost at the inverse order of heating rate.

1.5 Applications

Uncontrolled explosive boiling can be a serious threat to many industrial processes. But when produced in a controlled manner, it has a range of interesting and practical applications. Some of the applications are briefly explained below:

1.5.1 Thermal Actuation in MEMS(Micro Electro Mechanical Systems)

Based on thermal expansion amplification principle, thermal actuation in MEMS devices is done. A small thermal expansion in one part of the device causes a large deflection in overall device.

1.5.1.1 Ink Jet Printing[9]
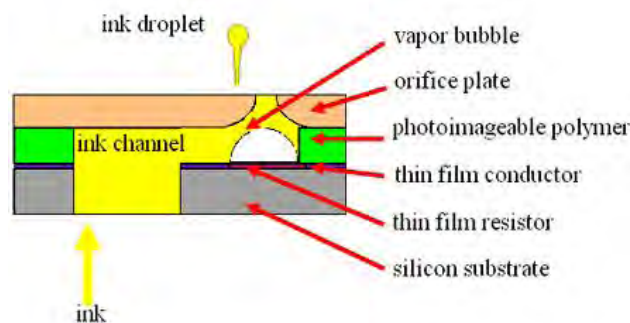
Fig. 1.2: Ink jet printing [10].

5

In a thermal ink jet printer (TIJ), the ejection chip is made of small components such as thin film resistors, drive resistors and micro channels fabricated via IC processing and silicon etching technology. Ink jet printing is based on a sequence of processes given below:

1. In a chamber, a thin film resistor in contact with the ink is present. An electrical current is applied to the resistor. The typical duration of the current is about 10 μs with a repetition frequency of 20 kHz [11]. The liquid in contact reaches very high temperature in a very short time and vaporizes at a temperature close to the superheat limit forming vapor bubbles.

2. The vapor bubbles then grow and displace the liquid away from the heater towards a micro nozzle, where a droplet of ink is ejected towards the desired substrate.

3. The chamber is automatically refilled with the ink and the system is ready to be actuated again.

1.5.2 Thermal Bubble in Micro-Fluidic Devices

For internal control of micro fluidic devices, an actuator mechanism of micro pumps and micro valves are used. For easier integration and larger stroke in this mechanism, actuation by thermal bubble is more preferable than piezo actuators [12].

1.5.2.1 Micro Valves
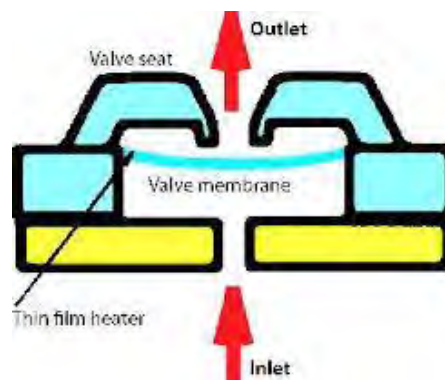
Fig. 1.3: Micro valves [13].

6

The working medium of typical thermo-pneumatic micro valve is surrounded by a volume in contact with a heater, which is separated by a membrane from the controlled flow by the valve. Actuating the heater induces an increase in volume of the enclosed system causing the membrane to deflect. Based on the application and required membrane displacements, working medium will vary. Substances that are used as membrane can be solid (paraffin), liquid (with or without phase change) or even a gas.

1.5.2.2 Micro Pumps

A chamber with a variable volume, inlet/outlet conduits with some rectifier valves to avoid reverse flow are found in a typical reciprocating micro pump. In a second chamber above the pump, working fluid is heated by a thin-film resistive element. The fluid expands due to heating and exerts pressure on the pump diaphragm forcing the liquid out of the chamber. The pump chamber is filled up with liquid after the heating of second chamber is stopped.
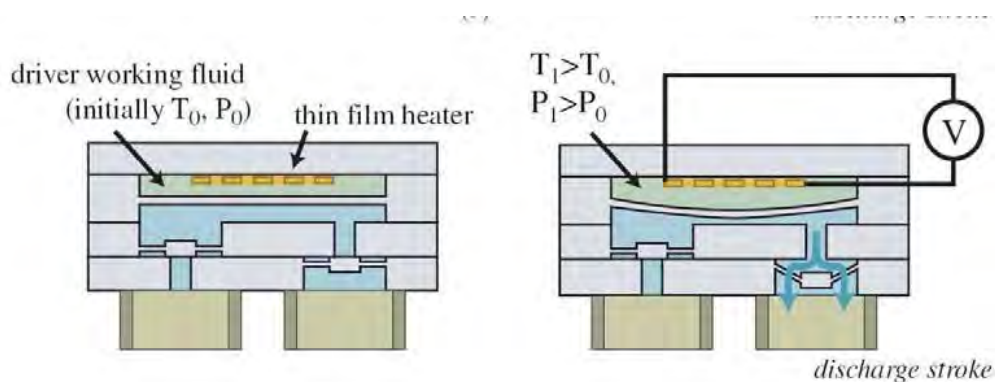
Fig. 1.4: Reciprocating displacement micro pump with thermo-pneumatic driver [14].

Micro pumps can also be valve less [15]. Instead of using rectifier valves, inlet and outlet of the pump make up a convergent-divergent nozzle pair with a preferred flow direction. This pair can easily be incorporated to micro fabricated system. Thermal bubble is found to be a useful actuation mechanism for such pumps [16, 17].
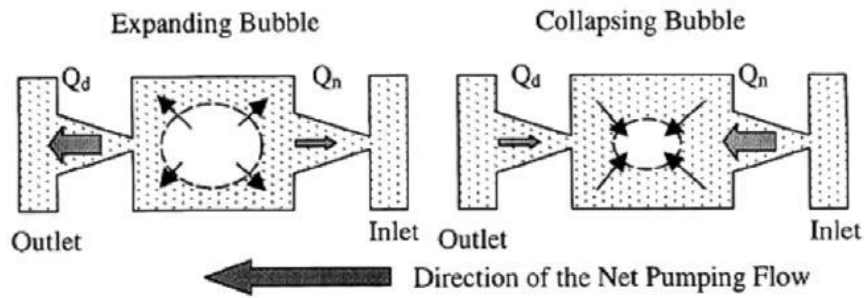
Fig. 1.5: Valve less nozzle-diffuser reciprocating displacement micro pump with thermo-pneumatic actuation [16].

In an interesting example of a micro pump actuated by the thermal bubble has been proposed by Yin and Prosperetti [18], an array of heaters is arranged on a quartz substrate along a micro channel. The heaters are actuated sequentially, starting with the closest to the inlet to produce peristaltic movement of the liquid.

1.5.2.3 Control of Biological Particles
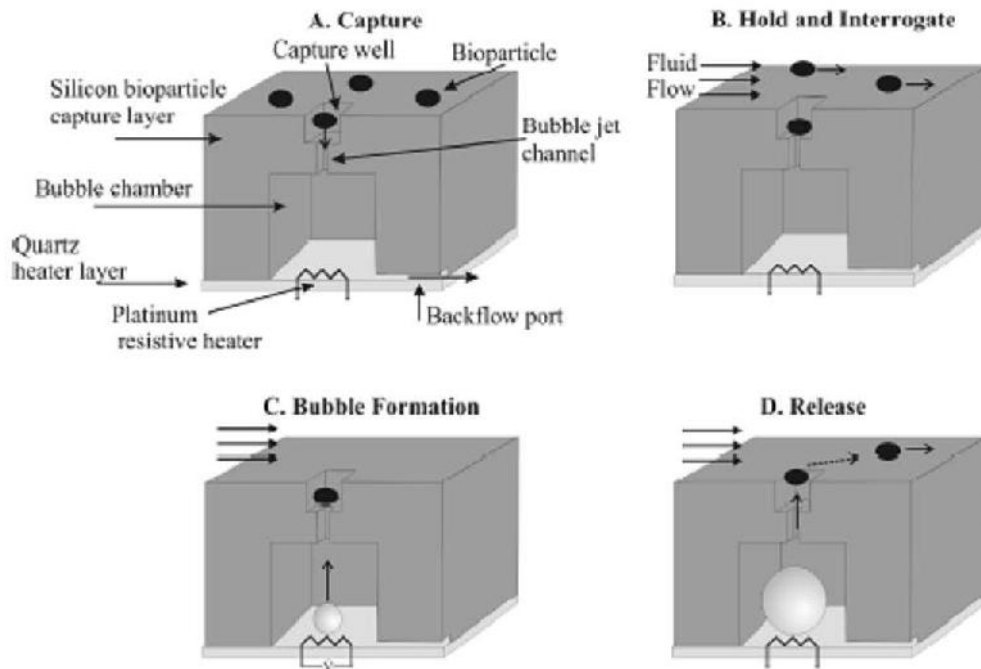
Fig. 1.6: Control of bio-particles using thermal bubble [19].

For controlled movement of particles in chemical and bio-chemical micro reactors, thermal bubbles are utilized. The mechanism is shown by Maxwell et al. [19]. In this mechanism, on the bottom of the micro channel a well is machined, which connects with a larger chamber by a duct. A thin film micro heater is placed on the bottom of this large chamber. Applying back pressure, bio particle is drawn to the well and then a back flow sweeps away the remaining particles. To release the particle from well, it is heated with micro heater to form a bubble and the volume expansion of bigger chamber exerts a jet of fluid which frees the bubble. Then it is entrained in the flow and carried away.

1.5.3 Thermal Bubble in External Flows

For precise control of external flows from various devices, actuation by thermal bubbles is very effective. To optimize low pressure atomization, thermal bubble actuation is highly suitable [20, 21].

1.5.3.1 Micro Fuel Injector

Fig. 1.7: Micro Fuel Injector. [21]

To ensure fast mixing with the oxidizer in the combustion engine, fuel is required to be injected in small uniform droplets. Typical injector systems use high pressure injection through a nozzle to produce droplets of sizes ranging from 10 to 100 μm diameter. They are conceptually very similar to the ink ejectors used in ink jet printing. Since there is high pressure cycling on the nozzle, micro injectors will allow for reduction of the stresses with more uniform droplet size which depends on the nozzle diameter. The operating frequency could reach 10 kHz.

1.5.3.2 Micro Thrusters
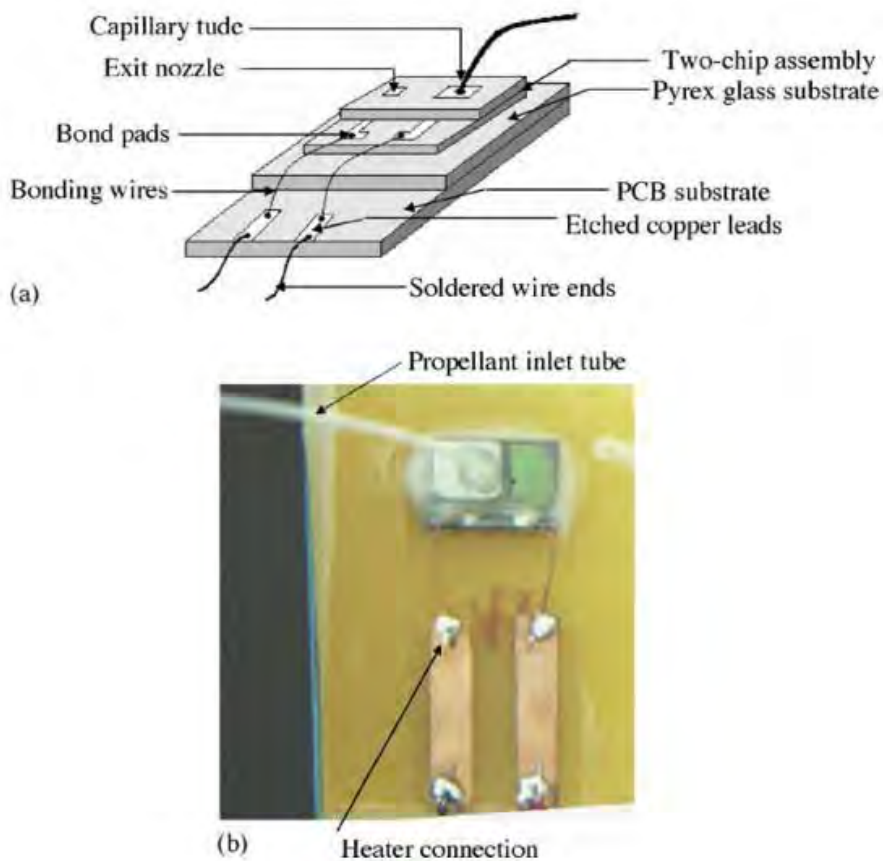
Fig. 1.8: Schematic view and microphotograph of the VLM test device [22].

For fine positioning of micro satellites, Vaporizing Liquid Micro thrusters (VLM) have been proposed by Maurya et al. [22]. The design consists of a propellant inlet channel, the vaporizing chamber with an integrated heater and a nozzle outlet.The liquid propellant enters the chamber and it is vaporized. The vapor escapes the chamber through a nozzle producing thrust.

1.5.3.3 Optical Switching
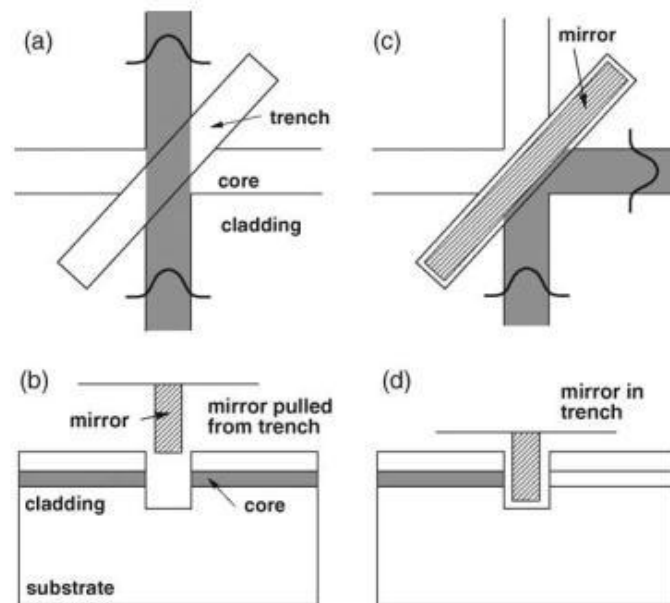
Fig. 1.8: Operation of an Optical Switch. (Crossbar Switch) [23].

One of the most promising applications of MEMS has been optical switching. By integrating micro actuator with planar optical fiber, a simple micro electromechanical optical switch can be formed. General technology associated with optical MEMS switch is based on micro mirrors combined with aligned optical fibers. These micro mirrors made of silicon or metal films are forced into or off the cross point of fiber axis. As the fiber is coupled with a gap of space in the switches, lack of wavelength structure could cause a high transmission loss. Therefore many researchers are focusing on new designs and optimized solution of optical switches [23]. In such researches, thermal actuation has been proposed for optical switching processes. In the cross point, liquid of required index of refraction fills the trench and the light travels straight through the liquid unimpeded. If a shift in direction is required, a bubble is formed and the light reflected off the interface of glass wall and the bubble to a new direction [24]. Another way is to use an air bubble trapped in a trench that can be pushed in the way of the light. The air bubble can be displaced in and out of the cross point [25].

1.6 Motivation of The Study

Explosive boiling or boiling explosion, which results from liquid superheating, has been present in many industrial and natural processes. Due to its destructive nature, the earlier research works centered on the conditions at which it will occur and the mechanisms associated with it. For sufficiently faster liquid heating cases, Skripov [26] reported that the liquid boiling was due primarily to random density fluctuation or homogeneous nucleation. Asai et al. [27,28] developed an analytical model for the bubble generation due to spontaneous nucleation or homogeneous nucleation followed by instantaneous formation of a vapor film, rapid bubble growth and cavitation bubble collapse during rapid liquid heating. Iida et al. [29, 30] concluded that bubble generation during rapid liquid heating is primarily due to spontaneous nucleation or homogeneous nucleation. Similar results have also been reported by Okuyama et al. [31], Zhao et al. [32] and Glod et al. [33]. Recently, Hasan et al. [34] has developed a theoretical model to predict the homogeneous boiling explosion condition under non-equilibrium heating condition. A number of experimental and theoretical studies have been published on the explosive nature of phase transition of different liquids (water, ethanol etc.) under various heating conditions, but our understanding on the limiting condition for boiling explosion is still inadequate. In experimental studies, determination of the actual moment when the boiling explosion occurs becomes difficult due to small time and space scales of the phenomenon. However, a well assessed theoretical model can predict the occurrence of the boiling explosion phenomena leading to better understanding of the limiting condition which triggers the phase change phenomenon in meta-stable liquids under non-equilibrium conditions. The motivation of present study is to find the characteristics of explosive boiling in ethanol at atmospheric pressure during isobaric rapid linear boundary heating and during contact with high temperature solid. Also this study targets to find out a novel criterion for the occurrence of homogeneous boiling explosion from an energy point of view i.e. how much energy is necessary to trigger the homogeneous boiling phenomena during non-equilibrium heating, which is independent of the initial condition.

1.7 Objective of The Study

As explosive boiling or boiling explosion has very small time and space scale, it is very difficult to ascertain the exact moment of its occurrence in experimental approaches. Therefore, a theoretical approach has been adopted to explore this phenomenon. Most of the researches conducted on explosive boiling till dates have been based on steady and equilibrium consideration. But practical heating cases are unsteady and non-equilibrium processes irrespective of the conditions. Therefore, new ideas and concepts are required for studying practical liquid heating. The specific objectives and outcomes of the research work are as follows:

(a) To model the liquid heating and subsequent boiling explosion processes considering finite liquid cluster at the boundary based on the principle of heat conduction and homogeneous nucleation.

(b) To investigate the effect of liquid cluster size on the prediction of homogeneous boiling explosion condition and hence to find out an appropriate size scale for the study of homogeneous nucleation phenomena under non-equilibrium heating.

(c) To find the characteristics of homogeneous nucleation boiling in ethanol in terms of average liquid temperature rise inside finite liquid cluster, maximum attainable cluster temperature and the time required to achieve the boiling explosion condition for different boundary heating rates.

(d) To investigate the effect of liquid boundary heating rate and liquid initial temperature on the time and temperature at the boiling explosion.

(e) To find out a novel criterion for the occurrence of homogeneous boiling explosion from an energy point of view

The experimental and theoretical studies, reported in the literature, on boiling explosion phenomenon do not provide us with any understanding of the limiting condition, which causes explosive phase transition of the metastable liquids during non-equilibrium heating. This study aims to address the limiting conditions that trigger the boiling explosion phenomenon which is irrespective of liquid initial and boundary conditions.

13

1.8 Thesis Outline

Explosive boiling resulting from liquid superheating has been investigated in this thesis and a novel criterion for explosive boiling has been found. The content of this thesis can be divided into following chapters:

Chapter 1:   It contains an introduction of the explosive boiling phenomena. The motivation and objectives of the present study have also been presented in this chapter.

Chapter 2:   A comprehensive review of earlier research works done on boiling explosion phenomena have been presented in this chapter.

Chapter 3:   A theoretical model used tosimulate the boiling explosion phenomena have been described in this chapter.

Chapter 4:   The applied model has been validated against some experimental micro scale boiling explosion observations in this chapter. The novel criterion for explosive boiling has also been described in this chapter.

Chapter 5:   In this final chapter, the concluding remarks have been delineated.

CHAPTER 2

LITERATURE REVIEW

2.1 Introduction

Omnipresence of boiling explosion due to liquid superheating is noticed in various industrial applications as well as in natural phenomena. Because of its potential to cause disastrous accidents, focus of earlier studies on this phenomenon was to understand the conditions at which boiling explosion occurs. But the advancement of micro scale science and technology, especially, the rapid development in Micro Electric Mechanical System (MEMS), has drawn the attention of researchers towards controlling micro-scale boiling explosion. Extraction of work from high pressure rapidly expanding vapor bubbles generated by this phenomenon could revolutionize the design and performance of MEMS machines. To search the applications of boiling explosion, understanding basic micro-scale boiling is important. Cases in which the time scale or space scale is reduced to a certain extent, some event occurs, that cannot be explained by classical heat transfer theory, and the associated boiling with these events differs from usual nucleate boiling in many aspect. First, origination of bubble nucleation is at a higher temperature around the theoretical superheat limit. Second, the boiling process is much explosive due to very high initial bubble pressure. Third, since the mechanism of the process is mainly governed by the property of the liquid (i.e. homogeneous nucleation) rather than by the surface characteristics (i.e. heterogeneous nucleation), the boiling process is more reproducible. That is why, micro scale boiling explosion has become one of the most sought-after topic in the field of heat transfer research. For a better understanding of the fundamental science and mechanism of boiling explosion phenomena, significant efforts are being given. The researchers are studying micro scale boiling explosion, both experimentally and theoretically. A concise description of such experimental and theoretical research works done on the boiling explosion with different liquid heating conditions has been presented in this chapter.

2.2 Experimental Studies

Impact Boiling or Boiling Explosion is a transient boiling phenomenon. Researchers have mostly tried to study this phenomenon experimentally. They have tried to understand the mechanism and conditions of the event by using different heating techniques (thin wires, thin-film micro heaters, high energy laser beams etc.). They have also focused on boiling explosion that occurs

during mixing of volatile cold liquid after coming in contact with non-volatile hot liquids or when liquid becomes superheated from contact with preheated solid surface. A short review of these researchers works are given below:

2.2.1 Research on Boiling Explosion Using Ultra Thin Heating Wires

In the earliest phases of research works on transient boiling phenomena such as, boiling explosion, to generate the event in experiment, fine platinum wires subjected to pulse heating were extensively used where the temperature of the wire was determined by the principles of resistance thermometry.

In one of the earliest work to date, Skripov [26] talked about explosive boiling phenomena of liquids under rapid heating for two typical processes - *Bulk Heating* which is the process of liquid heating by intense infrared or laser radiation and *Boundary/Surface Heating* which refers to rapid heating of dissolved electrolytes or immersed metal wire by an electric current. By performing transient boiling experiments on a fine wire under rapid heating in organic liquids, authors indicated that it is possible to superheat a liquid to its homogeneous nucleation temperature, where the molecular energy fluctuations become the dominant mechanism for vapor generation. The conditions of explosive boiling were defined as the minimum heating rate necessary to induce in the liquid to achieve the kinetic limit of liquid superheat. This condition was named as the Impact Boiling Condition. At lower heating rates than Impact Boiling Condition, some pre-existing nucleation centre may be activated, resulting in the boiling at lower degree of superheat. Their experiments [35] demonstrated that, for homogenous nucleation, required heating rate around a platinum heating wire immersed in water at atmospheric pressure was greater than 6.0×10^6 K/s.

Derewnicki [36] used a thin platinum wire of 25 μm in diameter under slow and rapid pulse heating at various system pressures to study transient boiling in water. In this study, at a slow heating rate, temporal temperature variation of the platinum wire was observed before nucleation. This temperature variation followed the theoretical solution for transient heat conduction and was independent of system pressure. At atmospheric pressure, the bubble nucleation temperature for slow heating rate of about 9.0×10^5 K/s was noted to be about 200 °C and only few active heterogeneous nucleation sites were found. On the other hand, for rapid

heating rate of about 6.0×10^6 K/s, the bubble nucleation temperature was obtained to be around 300 °C that was observed to be relatively independent of the system pressure.

Glod et al. [33] investigated the explosive vaporization by heating a platinum wire of 10 μm in diameter and 1 mm in length immersed in water. The bubble nucleation was observed to be originated by a single vapor bubble growing from a cavity on the wire surface at a slow heating rate of 10^5 K/s. This event subsequently triggered the boiling on the entire wire surface with heterogeneous nucleation as the main mechanism. It was notable that the nucleation temperature increased with the heating rate until a maximum limit is reached. At the maximum heating rate which is 86.0×10^6 K/s, the wire surface became almost instantaneously covered with a thin vapor film obtaining maximum nucleation temperature of 303 °C with homogeneous nucleation as main mechanism. From the acoustic pressure wave as a function of time, they calculated the useful extractable mechanical work.

2.2.2 Research on Boiling Explosion Using Thin Film Micro Heaters

With the advancement of MEMS technology, fabricating poly-silicon film micro heaters with its surface totally free of noticeable cavities in micron or even submicron scale have become a reality, which resulted in the applicability of much higher heat flux from heater surface.

Asai et al. [28, 37–38] investigated the boiling of water based ink and methyl alcohol occurring on small film heaters under high heat flux pulse heating condition. After performing a chain of theoretical and experimental studies on bubble nucleation and growth for typical operating condition of thermal ink jet printer, they gave a one dimensional numerical model of bubble growth and collapse and the resulting flow motion on a normal bubble jet printing head of effective heating area 150 μm × 30 μm. The proposed model [37] had two stages. In the first stage, which was the state before bubble nucleation, one dimensional heat conduction was approximated as the heat transfer process. At the second stage, the bubble nucleation process in water based ink happened about 270 °C by spontaneous or homogeneous nucleation which was around the experimentally obtained superheat limit of water. It was observed that bubble pressure decreased drastically from an initial value of about 4.5 MPa to less than 10 kPa in 10 μs. They also investigated the effect of ink viscosity and nozzle outlet length on the bubble

formation process for three different operating voltages. Another theoretical model presented by Asai [38] predicted the nucleation process in water based ink. Nucleation probability was derived in this model, and was utilized to simulate the initial bubble growth process. Model prediction was in good agreement with experimental results obtained from a prototype bubble jet printing head of effective heating area 150 μm x 30 μm for heat fluxes ranging from 100 MW/m^2 to 200 MW/m^2. From this model, the incipient boiling time was found as a random variable which became more reproducible as the heat input was increased. For powerful reproducible bubble formation, a sufficiently large heat flux (~ 100 MW/m^2) and threshold heat pulse duration were referred by Asai [38]. The author [28] proposed another model of bubble dynamics under high heat flux pulse heating conditions which was validated by experimentation using a thin film heater (100 μm × 100 μm) for methanol heating with high heat fluxes ranging from 5 to 50 MW/m^2. Based on the strong correlation between experimental result and theoretical prediction, the spontaneous nucleation of liquids due to thermal fluctuation i.e. the homogeneous nucleation was suggested as the dominant bubble generation mechanism.

Thermal microbubble formations with line shape polysilicon resistors with a typical size of 50 μm × 2 μm × 0.53 μm, were experimented by Lin et al. [39]. Various fluids such as Fluro-inert fluids, water and methanol were used in their experimental study. Important experimental phenomena such as Marangoni effects in micro scale, controllability of the size of microbubbles, and bubble nucleation hysteresis were described. A one dimensional electro-thermal model was also developed by them to investigate the bubble nucleation phenomena. Both the experimental observation and the developed electro-thermal model indicated the bubble formation on the microheater occurred because of homogeneous nucleation.

A small platinum film heater (effective heating area of 100 μm × 400 μm), which allows simultaneous precise measurement of heater temperature, was used in studies conducted by Iida et al. [29–30]. These studies commented on the boiling nucleation phenomenon in various liquids (ethyl alcohol, toluene and water) occurring at high boundary heating rates of up to 9.3 ×10^7 K/s. Saturated value of heater temperature at the boiling incipience was detected at approximately 1.0 ×10^7 K/s for ethyl alcohol & toluene and at approximately 4.5 ×10^7 K/s for water. For ethyl alcohol, the obtained value agreed well with the homogeneous nucleation temperature. They also noticed the immediate generation of many uniformly sized tiny bubbles after the boiling incipience, and the number of bubbles tended to increase as predicted by the

homogeneous nucleation theory. From the obtained results, they reached the conclusion that bubble generation during rapid liquid heating is due primarily to spontaneous nucleation or homogeneous nucleation.

Both Iida et al. [40] and Okuyama et al. [41] examined the mechanism and associated heat transfer characteristics of spontaneous boiling process for ethyl alcohol by varying the system pressures and liquid temperature. During these experiments, the heat transfer rate did not significantly increase in spite of the simultaneous generation of huge number of fine bubbles. A vapor film covered the entire surface by prompt coalescence of these fine bubbles, which was followed by a noticeable decrease in heat transfer. The vapor film then rapidly expanded into a single bubble. This bubble shrank and collapsed with a significant increase in heat transfer at the collapse. The time variation of the bubble shrinking and collapsing was found to be dependent on the liquid heating rate from the early stages of the heating to coalescence, regardless of the continuation of the heating after coalescence. With the increase of the system pressure and the decrease in the liquid bulk temperature, the lifetime of the bubble was observed to be shortened considerably.

Okuyama et al. [31] further studied on the dynamics of boiling process following the spontaneous nucleation on a small film heater (0.1 mm × 0.25 mm) immersed in water and ethyl alcohol for much higher boundary heating rates ranging from 10^7 K/s to approximately 10^9 K/s. After experimenting in these extreme liquid heating conditions, they observed the spontaneous nucleation to be dominant for the inception of boiling. After simultaneous generation, large number of fine bubbles forms a vapor film by immediate coalescence that rapidly expanded to a single bubble. The coalesced bubble was found to become flatter with the increase of the heating rate, and only a thin vapor film was noticed to grow before cavitations collapse.

Avedisian et al. [42] investigated homogeneous nucleation with a Ta/Al heater (65 μm x 65 μm). A SEM examination of the surface structure of the micro heater showed that there was no surface imperfection for nucleation sites on the heater surface. They measured the average temperature of micro heater on a silicon substrate of a commercial thermal ink jet printer (TIJ) which was immersed in subcooled water during pulse heating at microsecond duration. An inflection point on the temperature profile of the heater surface was identified as the nucleation temperature. They noted that the increase of bubble nucleation temperature with the heating rate and at a

maximum heating rate of 2.5 $\times 10^8$ K/s, it approached a maximum value of 270 °C. Also, for an appropriate value of the contact angle, the values of nucleation temperatures were found to be in qualitative agreement with the prediction of homogeneous boiling theory. It was observed that the homogeneous nucleation temperature increased with the liquid heating rate until approaching a constant value.

Zhao et al. [32] experimented on thin film heaters (100 μm × 110 μm) immersed in water at atmospheric pressure to determine the presence of explosive boiling process and measured the pressure transients generated by exploding micro vapor bubbles. Soon after the beginning of the explosive vaporization, the acoustic pressure emission was found to increase linearly with time. It was also observed that the largely generated vapor volume, from the microscopic vapor explosion, was found to have a typical linear dimension of about 100 μm. The maximum expansion velocity of the vapor layer on the micro heater surface was found to be 17 m/s while the pressure inside the vapor volume was calculated to be about 7 bars. Using these measurements, they attempted to quantify the amount of mechanical work released to the surrounding liquid during boiling explosion.

Guereca et al. [43] investigated the heating and boiling phenomena triggered by a submicron thin film strip platinum heater (>1 μm × 3–6 μm) subjected to pulsed heating in water. They observed that the time lag between heating onset and boiling incipience is inversely proportional to an increase in the intensity of the supplied current and increases the boiling temperature. The temperature evolution of the heater showed a rapid transient behavior followed by a temperature plateau. They found consistent high frequency oscillation in the temperature curve in the plateau region for different intensities of supplied current. Based on the obtained results, they concluded that the temperature oscillation in the plateau region is caused by the counteracting effects of the heat supply to the interface by the heater and the heat removal by the cooling effect of the sub-cooled bulk liquid.

For pulse widths of 1–10 ms duration at different heat fluxes between 3 and 44 MW/m^2, Yin et al. [44] studied the bubble nucleation process in FC-72 on an impulsively powered square micro heater (260 μm × 260 μm). It was seen in the study that the bubble growth occurs rather violently, then followed by a rapid shrinking of the vapor mass and a subsequent slower expansion. At a low heat flux of 3.43 MW/m^2, there was a consistent nucleation of a single large

bubble near the center of the heater which grew forcefully exceeding its equilibrium size, then shrinked, and stabilized over the heater. At the high heat flux of 44 MW/m^2, nucleation occurred at several spots on the heater. The nucleation temperature was reached much earlier and there was insufficient time to heat up a substantial mass of liquid. But after the heater had been turned off, the heat stored in the solid substrate was observed to play an important role in the secondary vapor growth.

The bubble nucleation in dielectric liquids (such as FC-72, FC-77 and FC-40) heated by polysilicon micro heaters (50 μm × 3 μm and 50 μm × 5 μm) under steady or finite pulse of voltage input was investigated by Jung et al. [45]. It was obtained that the bubble nucleation temperature on the heater with 5 μm width was considerably lower than the superheat limit, while the temperature on the thinner width of 3 μm was higher than the superheat limit.

A series of experiments under pulse heating conditions, using thin film planar platinum heater of non-uniform width with the narrow part ranging from 0.5 μm to 70 μm was carried out by Deng et al. [46] to investigate micro vapor bubble generation. A voltage pulse of 1.66 ms duration was applied on each platinum heater, while the height of the voltage pulse was increased from zero until boiling was observed at certain voltage which established for each heater the minimum power input to induce the boiling was at this pulse width. The beginning of bubble nucleation temperature was measured using each platinum heater as a self-sensing resistive temperature sensor. The bubble nucleation process was visualized by a high-speed CCD (Charge-Coupled Device) camera, and a 100 MHz high-speed digitizer was used for data acquisition. For a critical dimension of the micro heater (10 μm), they observed single spherical bubble generation with heater's feature size less than 10 μm while they observed oblate vapor blanket on the heater surface with the size larger than 10 μm. It was found that scaling effect of the heater could greatly affect the boiling pattern.

Kuznetsov and Kozulin [47] studied the explosive vaporization of a water layer under pulse heating condition on micro-heater (100 μm × 100 μm) with a surface coated with a sub-micron silicon carbide layer using an optical method based on measuring the intensity of a laser beam mirrored from the heater surface. They focused on the dynamics of the filling the heater surface with the vapor phase and the lifetime of the main vapor bubble and the satellite bubbles. From recordings of time history of the vaporization process and the dynamics of the steam blanket

generated on the heater surface for a maximum heater temperature rising rate of about 1.80×10^8 K/s, the experimentally observed temperature of the beginning of explosive vaporization was found to be lower than the spinodal temperature. The reason given by the author was the decreasing work of boiling nucleation near the silicon carbide surface.

Xu and Zhang [48], studied the effect of pulse heating parameters on the micro bubble behavior of a platinum microheater (100 μm × 20 μm) immersed in a methanol pool with heat fluxes of 10–37 MW/m^2 and pulse frequency of 25–500 Hz. The boiling incipience temperature was found as the superheat limit of methanol, corresponding to the homogeneous nucleation.

Using stroboscopic visualization technique with a time resolution of 100 nsec, Varlamov et al. [49] observed explosive boiling of liquids (water, toluene, ethanol, and isopropyl alcohol) on film heaters under the action of pulsed heat fluxes of 100–1000 MW/m^2. They discovered the specific conditions of thermal effect (magnitude of heat flux, duration and repetition frequency of the heat pulse) which ensure single and repeated boiling, intermittent boiling, and boiling with formation of complicated multibubble structures. Comparing their theoretical predictions with experimental data, a conclusion was drawn that homogeneous nucleation was the dominant mechanism for boiling in all liquids under consideration for heat fluxes higher than 100 MW/m^2.

Hong et al. [50] experimentally studied the rapid formation and collapse of bubbles formed on a microheater (25 μm × 80 μm) induced by pulse heating. A high heat flux pulses of more than 750 MW/m^2 was applied to the resistive heater while the pulse heating duration ranged from 1 μs to 4 μs. They found a threshold pulse duration above which the maximum size of the bubble does not change anymore. It was also observed that the time of nucleation did not change with the liquid initial temperature, but the maximum bubble size increases with an increase in the liquid initial temperature. Nucleation temperature for water obtained from experiments was slightly below the theoretical superheat limit and had a weak linear dependency on the heating rate. They mentioned the mechanism of the bubble formation to be a combined homogeneous-heterogeneous nucleation.

A model for identification and simulation of the dynamics of bubble and liquid flow in the thermal pneumatic micro actuator (60 μm × 60 μm) of thermal ink jet was given by Rembe et al. [51]. Positions of the ejected liquid column and the velocity of the ejected ink from the nozzle were measured from the sequence of images captured by stroboscopic technique. A dynamic

equation of the liquid column exiting from the nozzle in terms of the vapor pressure was obtained by employing mass balance and force balance. By considering thermal diffusion in the heater and liquid, the thermodynamics of the bubble, and the conservation of the energy along with the dynamic equation, a state space representation of non-linear differential equations by using integral method derived was derived by the authors. They solved the state representation numerically to obtain the temperature in the bubble and the movement of the liquid column. They also discussed the effect of higher ambient pressure on the movement of the ejected liquid.

Another numerical study by Chen et al. [52] simulated the bubble generation and ink ejection process of a thermal ink jet print head with a thin film heater (65 μm × 65 μm), in which using one-dimensional heat conduction model and the theories presented by Asai [28], they obtained the bubble volume, temperature and pressure at various operating voltages. They observed that the bubble volume decreases with increasing voltage. They also derived the relationship between threshold voltage and the pulse duration, where the defined threshold voltage is the minimum voltage that could generate enough heat for bubble nucleation at the end of the heating pulse.

From the experiment conducted by Andrews and O'Horo [53] it was seen that rapid transient heating of a film heater in contact with liquid produced some bubbles by heterogeneous nucleation and some bubbles by homogeneous nucleation. A particularly interesting observation was about the bubble formation by homogeneous nucleation away from the heater surface. This event was in contradiction with the expectation that homogeneous nucleation would have to take place first at the surface itself where the liquid being the most superheated.

Carey and Wemhoff [54] argued against the observation made by Andrews and O'Horo [53], by stating that there would have been a mechanism that suppressed the homogeneous nucleation very near the heater wall. They mentioned one possibility of modifying the intrinsic stability limit of liquid by some force interactions between molecules of the liquid and molecules in the solid surface that might affect the state of the liquid. Earlier, in the analytical model of the effects of attractive forces on the equation of state of the fluid by Gerweck and Yadigaroglu [55], they followed a thermodynamic analysis to assemble an equation of state by combining a repulsive force interaction model for a hard sphere fluid with attractive force models for interactions between fluid molecules and solid surface molecules. Forming the analysis in terms of an inverse characteristic length they concluded that the characteristic length scale was of the order of a few

molecular diameters but no specific value was mentioned. Carey and Wemhoff [54] developed a thermodynamic model from the interesting insight of Gerweck and Yadigaroglu [55] and suggested that near-wall effects of nucleation and boiling are confined to the region of few nanometers from the surface where the local pressure and the spinodal limit are extremely high. They [54] also obtained a very good agreement between their model results and the experimental observation made by Renbe et al. [51], for identical liquid initial and heating conditions.

2.2.3 Research on Boiling Explosion Using High Energy Laser Irradiation

Using high-power nanosecond Nd: YAG laser pulse, Ueno et al. [56] investigated the nucleation and pressure generation on an irradiated solid silicon surface in water. Approximately 10–20 ns after the onset of irradiation bubble formation occurred with bubble radius in the order of 80 nm. A shockwave in the order of 1 MPa was recorded during experimentation. They compared the period from heating onset to bubble formation with the time required for the solid surface to reach the homogeneous nucleation temperature via heat conduction.

Huai et al. [57] observed explosive vaporization process induced by firing a micro second pulsed laser beam on a thin Pt film deposited on a quartz substrate. These experiments were carried out in either a pool of acetone liquid or athin acetone film covering the Pt film. The bubble formation and the explosive evaporation process were visualized by employing a high-speed photographic technique. The heating rate was ranged between 8.0×10^6 K/s to 9.0×10^7 K/s. In the case of a liquid film, intense explosive boiling was observed and the vapor bubbles together with liquid droplets were ejected from the Pt film, while in the case of aliquid pool, only a large cluster of bubbles was formed on the Pt film during laser heating. A close examination of the temperature curves showed a sudden reduction in the heating rate during laser heating and an apparent bubble nucleation temperature was defined, which is a strong function of the heating rate demonstrated by experimental data. At low heating rates, it was close to the equilibrium boiling point while approached the homogeneous nucleation temperature at considerably high heating rates.

In another experimental study performed by Huai et al. [58], rapid transient explosive boiling of mixed ethanol and acetone of different volume fractions were investigated. A platinum film heater in the test liquid was irradiated by pulsed Nd: YAG laser with a wavelength of 1.06 μm

for different pulse durations ranging from 1 to 30 μs. The spot diameter was varied from 1 to 10 mm and the maximum power density was obtained up to 10^4 MW/m^2. A microscopic camera system was used to observe the behavior of bubbles including their formation, growth, and departure etc. The intensity of explosive boiling or the number and the floating velocity of bubbles were noticed to depend on the laser power, the pulse duration and also the property of the liquid. The explosive boiling was found to be less volatile with more fraction of the high boiling point liquid in the mixture. It was also found that the bubble nucleation temperature depends strongly on the heating rate.

Some results of numerical calculations of water-droplet explosions initiated by intense CO_2-laser radiation were demonstrated by Geints et al. [59]. Based on the solution of the thermal-boundary problem in a homogeneously heated droplet, including the kinetic equation describing vapor generation in a superheated liquid, the theoretical model for this process was devised. The main characteristics of droplet explosions (e.g., degree of explosive evaporation and time of explosion) were calculated. It was shown that these characteristics depend on the heating rate of the droplet and on its radius. The obtained results indicated two distinguished droplet-heating regimes for slow heating and rapid heating-based on the behavior of the explosive boiling process.

2.2.4 Research on Boiling Explosion during Liquid Mixing with Hot Non-volatile Liquid and Boiling Explosion upon Liquid Contact with Hot Surfaces

In metal processing industries, two fluids of different temperatures may come in contact with each other. If the hotter liquid is non-volatile (smelt or molten metal) and the cooler liquid is comparatively volatile (water or refrigerant), the later can be superheated to the point, that boiling explosion occurs and can injure personnel as well as cause severe structural damage.

Depending on the speed of the heat transfer between the two liquids, Henry and Fauske [60] noted two types of vapor explosions - large and small scale vapor explosion. In large scale vapor explosion, two liquids having large temperature difference are mixed and the speed of heat transfer is comparable or less than the acoustic relief time of the liquid-liquid system. While in case of small scale vapor explosion, temperature difference between liquids are small and heat is

stored within the cold liquid on a time scale larger than the acoustic relief time. A spontaneous nucleation model was suggested to describe the inception and propagation mechanisms for vapor explosions. Recognized by Henry and Fauske [60], the essential conditions for an explosive boiling for liquid-liquid systems are: (i) the threshold temperature for spontaneous nucleation in the cold liquid, (ii) the existence of stable film boiling to sustain vapor embryos of the critical size prior to boiling explosion, (iii) the size of cold liquid drops exceeding a critical value to be captured by the hot liquid surface, and (iv) the interfacial temperature between the two liquids exceeding the homogeneous nucleation temperature.

The destabilization of film boiling or the vapor film collapse as the mechanism of triggering and propagation of vapor explosion were observed by Inoue and Bankoff [61- 62]. They suggested a decrease in the hot or cold liquid temperature (or both), an increase in the relative velocity of the two liquids, or by a sudden increase in pressure favor destabilization.

Ochiai and Bankoff [63] recommended the 'splash' theory, which states that splash (instantaneous boiling or vapor explosion) occurs at the interfacial temperature between the two liquids, T_i ranges between the spontaneous nucleation temperature, T_{sn} and the critical temperature of the cold liquid, T_{cr} ($T_{sn} < T_i < T_{cr}$).

By performing experiments on vapor explosions resulting from mixing of a molten salt drop such as LiCl or LiNO$_3$ in water, Iida et al. [64] found the necessary conditions for vapor explosion in the molten salt-liquid system. The conditions were stable film boiling and interfacial temperature, T_i being higher than spontaneous nucleation temperature T_{sn} ($T_i > T_{sn}$). They also observed that both the hot and cold liquids had the upper and lower temperature limits for vapor explosion.

The research works mentioned earlier, focused on the mechanism of boiling nucleation and growth, but research on the boiling phenomena upon liquid contact with a hot surface concentrates on the potential of exploding vapor to perform work on the surrounding bulk liquid. Earlier research on this subject has been performed with focusing on understanding the limiting condition at which a liquid can wet a hot surface. If the simplest case of pool boiling is considered, initial dry state & wet state corresponds to film boiling and nucleate boiling. Therefore, considered limiting condition has been described by scientist as the minimum film

boiling (MFB) temperature, minimum heat flux (MHF) temperature or the temperature of film boiling destabilization, the rewetting temperature, the Leidenfrost temperature etc.

The maximum superheat temperature of the liquid is the temperature above which the liquid would immediately boil explosively and thus could not touch the surface. Rewetting model proposed by Spiegler et al. [65] based on this maximum superheat temperature hypothesis considered that the rewetting will not occur in the liquid temperature at the contact point, T_i, that is the interface between the solid and the liquid, is higher than the maximum temperature the liquid can exist, T_{max}. The maximum superheat limit was considered as the spinodal limit obtained for the Van der Waals equation of state for the liquid which might be given as, $T_{\max} = (27/32)T_c$, where T_c is the critical temperature of the liquid. The infinite slab model, which considers that both the solid and liquid behave like two semi-infinite slabs of uniform initial temperatures that are suddenly brought into contact, was used to approximate the interfacial liquid temperature.

For the prediction of the temperature for film boiling destabilization and its relation with vapor explosion phenomena, Gunnerson and Cronenberg [66] suggested a thermodynamic model. Like Spiegler et al. [65], they considered the solid-liquid contact phenomena as a two 1-D semi-infinite body contact problem. This model identified the condition of boiling in both perfectly smooth and imperfect surfaces. Boiling was considered to occur at an interfacial temperature equal to the maximum liquid superheat, for a perfectly smooth surface. On the other hand, for imperfect interface, boiling was expected to occur at a minimum interfacial temperature equal to the liquid saturation temperature at the prevailing pressure. Viewing the Leidenfrost temperature as the minimum wall temperature for film boiling, a range of theoretical Leidenfrost temperature was recommended which are the wall temperatures at these two extreme situations for a particular solid-liquid combination.

The liquid to vapor transition process during liquid contact with a hot wall were investigated by Gerweck and Yadigaroglu [55]. Using statistical mechanics, they derived an approximate local equation of state for the fluid as a function of distance from the wall, reaching a wall rewetting condition different from the minimum film temperature. The definition of the rewetting temperature by them was the temperature at which the liquid can touch wall without being immediately turned into vapor. The immediate phase change identified in the investigation,

28

referred to the explosive vaporization of the liquid near the maximum liquid superheat. A conclusion was drawn that, the spinodal temperature be a good estimation for the maximum superheat temperature that a liquid can sustain on a wall, for most situations encountered in rewetting experiments.

Zhang and Yang [67] employed laser shadowgraphic and direct photographic methods to study thermal stability and flow structures during drop evaporation on a heated surface. The existence of four different flow regions was revealed in stable and unstable drops at low liquid-film type vaporization regime. When surface temperatures became higher, the flow regions were reduced to two. The micro explosion of drops was identified in the transition-boiling type heating range. But no drop explosion was found in the spheroidal vaporization regime except when the drop had rolled on to a micro scratch in the heating surface. From these observations, they reached the conclusion that the mechanism for triggering drop explosion includes the spontaneous nucleation and growth phenomena and the destabilization of film boiling.

Inada and Yang [68] experimented on the boiling phenomena of single water drops upon impingement on a heated surface. Using a high speed video camera, vapor micro explosions were captured. Measurements were made on the frequency and amplitude of the elastic longitudinal waves produced by boiling and the acoustic pressure of boiling sound by using a piezo-electric potential transformer and a condenser microphone respectively. For violent miniaturization of sessile drops, the maximum frequency and amplitude of the elastic-longitudinal waves and the maximum values of the boiling acoustic pressure to occur were found in a certain range of the surface temperatures. The range of the surface temperatures coincided with that of the transition boiling regime around the homogeneous nucleation temperature of the liquid. According to their report, the miniaturization phenomena was induced by an explosive boiling resulting from a direct contact between parts of the liquid and the heating surface. The analysis of their experimental data also revealed out the frequency of solid-liquid contact i.e. the frequency of bubble generation resulting from the liquid-solid contact might be in the order of 8–9 kHz.

2.3 Theoretical Study

There are two approaches to determine the superheat limit of liquid i.e., the maximum attainable temperature to which liquid can be heated before it spontaneously vaporizes. The first approach is based on the mechanical stability consideration of classical thermodynamics. According to this approach, superheat limit is the locus of minima in the liquid isotherms at constant pressure and composition i.e. the spinodal curve and satisfies the conditions $(\delta P / \delta V)_T = 0$ and $(\delta^2 P / \delta^2 V)_T > 0$. It indicates the deepest penetration of the liquid to the domain of metastable states and termed as Thermodynamic superheat limit or Spinodal limit, T_{TSL}. The spinodal curves separate the metastable state satisfying mechanical stability condition, $(\delta P / \delta V)_T < 0$ from the unstable region, $(\delta P / \delta V)_T > 0$. Liquid and vapor can stay in their respective forms indefinitely in both stable and metastable region where the local density fluctuations weaken with time. But in unstable region, even the smallest fluctuations grow and cause liquid or vapor to lose their form. Investigation of the calculated value of spinodal is done on the basis of different equation of state [69].
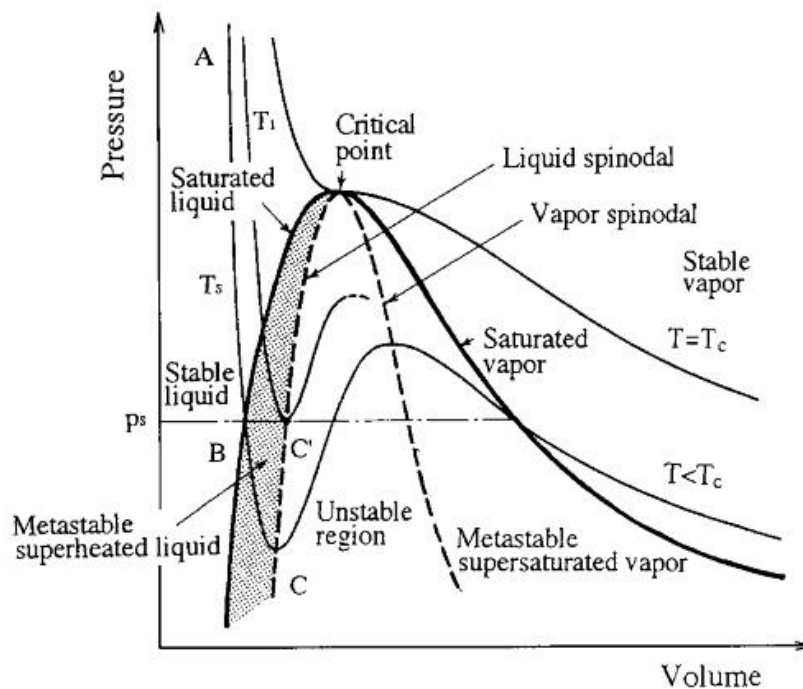
Fig. 2.1 Pressure- volume chart of fluid and the range of metastable superheated liquid [6].

For example, Spiegler et al. [65] deduced the condition for mechanical stability i.e thermodynamic superheat limit, T_{TSL} applying Van der Waal's equation of state, which was

$$T_{TSL} = 0.844T_C \qquad (2.1)$$

Where, T_c = Critical Temperature of Liquid

Lienhard [24] suggested following correlation for T_{TSL},

$$\left\{ \frac{(T_{TSL} - T_S)}{T_C} \right\} = 0.905 - \left(\frac{T_S}{T_C} \right) + 0.095 \left(\frac{T_S}{T_C} \right)^8 \qquad (2.2)$$

where, T_c = Critical Temperature (K) and T_s = Saturation Temperature (K).

The second approach to determine the superheat limit is by kinetic homogeneous nucleation theory [71-73], where temperature and pressure dependence of bubble nucleation are based on molecular fluctuation probability. Molecular fluctuation occurs at and above the saturation condition and induces a localized decrease in the liquid density, causing the formation of vapor embryo. Molecular fluctuation probability increase with temperature and at the superheat limit, probability of high bubble embryo formation rate, in other words, threshold nucleation rate is enough to transform the liquid to vapor. According to this approach, the superheat limit of liquid is named as homogeneous nucleation temperature or spontaneous nucleation temperature. As stated by classical homogeneous nucleation theory, the highest nucleation rate per unit liquid volume, J, for a liquid of temperature, T_l, is determined by following expression,

$$J(T_i) = N_l f \exp\left(-\frac{W_{min}}{k_B T_l} \right) \qquad (2.3)$$

where, N_l = Number density of liquid molecules; f = Frequency factor;

k_B = Boltzmann Constant; W_{min} = Free energy of formation of a critical nucleus.

Doing further simplification Carey [74] derived following homogeneous nucleation rate equation,

$$J(T_l) = N_l\sqrt{\frac{3\sigma}{\pi m}}\exp\left\{-\frac{16\pi\sigma^3}{3k_B T_l[P_{ve}(T_l)-P_0]^2}\right\}$$

(2.4)

where, σ = Liquid surface tension; m = Molecular mass of liquid;

P_0 = Bulk liquid pressure; P_{ve} = Equilibrium vapor pressure at given temperature.

To determine kinetic limit of superheat, equation (2.4) can be solved iteratively assuming a threshold value of *J* corresponding to the onset of homogeneous nucleation. Blander and Katz [73] obtained 10^{12} nuclei / (m³s) as a threshold value from experimental superheat data for large variety of fluids at atmospheric pressure. Carey [74] also suggested 10^{12} nuclei / (m³s) as threshold value. But according to Cole [75], 10^6 nuclei / (m³s) as threshold nucleation rate gives perfectly acceptable result for limiting kinetic superheat temperature in most situations.

Based on these two approaches to determine superheat limit of liquid, researchers have tried to model boiling explosion phenomena in parallel with the experimental studies. Some of their works are briefly discussed below:

2.3.1 Theoretical Modeling of Boiling Explosion in Superheated Liquid

When the limit of liquid superheat is approaching, complex thermal and mass transfer processes occur. To report these processes, Li et al. [76] presented a mechanistic model. In practical cases related to some MEMS applications, where a very small non-uniformly heated liquid volume might be present, a set of criteria for estimating the limit of superheat were formulated by the authors. For a non-uniformly heated volume of liquid, the suggested model was applied to estimate the spatial location and time for achieving the limit of liquid superheat.

A mathematical relationship between the lifetime of superheated liquid and its temperature was derived by Elias and Shusser [77]. To specify the temperature variation of the liquid during the nucleation process, the energy equation in conjunction with a non-equilibrium vapor formation model was solved and it was proved that the expectation time of a uniformly superheated liquid decreases with increasing temperature. The liquid superheat limit was defined as the liquid temperature above which boiling starts almost instantaneously. A good agreement between their model results and classical nucleation kinetic data was achieved.

Elias and Chambre [78] developed another model to simulate the complex heat and mass transfer process taking place inside a pure liquid subjected to intense heating. It was assumed that liquid heating occurs by a constant and uniform volumetric internal heat source. Formulating and numerically solving a heat balance equation, the liquid temperature curve and the evaporation rate up to the maximum attainable liquid superheat were found. The effect of liquid heating on the liquid temperature curve had been quantified. But for the non-uniform and transient heating cases, this model became inadequate as it does not take the size of the liquid volume under consideration.

Recently, Hasan et al. [79] developed theoretical model for the process of rapid, non-uniform transient liquid heating and subsequent boiling explosion in water. The proposed model predicted boiling explosion condition. The results are in good agreement with experimental observations of micro scale boiling explosion as reported in the literature and with the theoretical explosion condition corresponding to the maximum possible heat flux across the liquid–vapor interface, $q_{max,max}$, as proposed by Gambill and Lienhard [80] .

2.4 Summary

Both experimental and theoretical investigations under various liquid heating conditions regarding boiling explosion or explosive boiling are mainly focused on the mechanism of boiling initiation/nucleation and the effect of boiling phenomena on the surroundings. Almost in all of the research works, the conditions of explosive boiling have been interpreted in terms of equilibrium liquid heating conditions. Only a few studies considered boiling phenomena during non-equilibrium liquid heating but the size of the liquid volume being heated was not taken into account. Also, the exact moment at which boiling explosion occurs, is very difficult to determine experimentally. These theoretical and experimental studies do not provide us with understanding of the limiting condition which causes explosive phase transition of the metastable liquids during non-equilibrium heating. They are not adequate enough to understand the limiting condition which triggers the boiling explosion phenomenon, irrespective of liquid initial and boundary conditions.

CHAPTER 3

MACROSCOPIC MODEL FOR EXPLOSIVE BOILING UNDER NON-EQUILIBRIUM CONDITION

3.1 Introduction

The focus of previous studies on explosive boiling or boiling explosion mainly revolved around the incipience condition of bubble generation, the mechanism of boiling nucleation, and the effect of rapid oscillation of bubble growth and collapse on liquid motion and the heater involved. But the conditions of boiling incipience and that of boiling explosion are completely different. Explosive boiling is independent of liquid initial and boundary conditions and the limiting condition which triggers it, is yet to be identified. Experimentally, due to various practical limitations, it is very difficult to pinpoint the exact moment at which boiling explosion occurs, especially at extremely high rates of liquid heating. Theoretical model suggested by Elias and Chambre [78], simulated the boiling explosion condition for constant uniform liquid heating. But in practical cases, liquid heating is a transient and non-uniform process. As their model does not consider the liquid volume being heated, it is inadequate to handle transient non-uniform liquid heating. Therefore, to deal with explosive boiling that occurs in realistic transient non-uniform liquid heating cases, using a model that considers an appropriate liquid volume is crucial. Recently Hasan et al. [79] has developed a theoretical model by considering a finite liquid volume for the process of rapid, non-uniform transient liquid heating and subsequent boiling explosion. In the model following assumptions are considered,

1. Heating process for liquid cluster has been assumed as Heat Conduction for 1-D semi-infinite solid.

2. Thermo-physical properties of liquid are assumed constant except for vapor generation term.

3. Equilibrium state at the liquid-vapor interface has been considered

4. All vapor bubbles are assumed to grow independently after their generation.

For water, the model predictions are in good agreement with previous experimental studies discussed in the literature. The same model will be used for ethanol in the present study. It is briefly described below:

3.2 Energy Balance Equation

To demonstrate the energy balance caused by liquid heating in contact with a solid heater, a liquid cluster with a thickness, x_e, at the boundary ($x = 0$) has been considered as a finite size control volume in the employed model, which is shown in *Fig. 3.1*. Energy enters at x = 0 and a portion of it gets deposited within the control volume continuously at a rate of q_d (W/m^2).

A portion of deposited energy is added as sensible energy of liquid and raises the liquid temperature while the remaining portion contributes to the latent energy required for possible boiling at a rate of q_c (W/m^2). If x_e is significantly small, the average liquid temperature inside
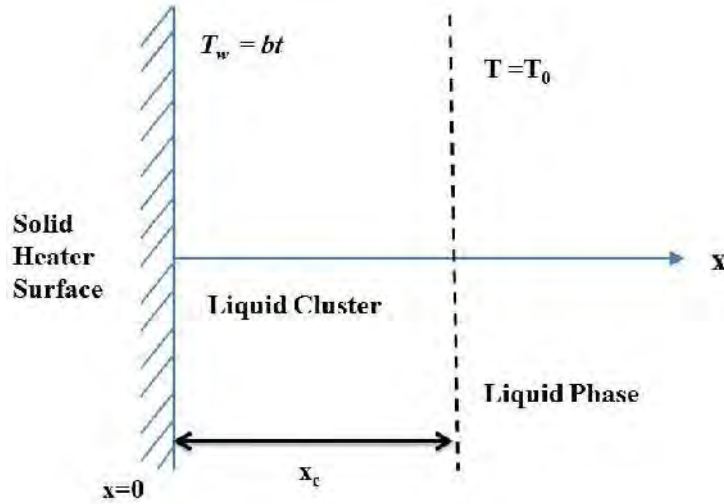
Fig. 3.1: Liquid control volume at the solid-liquid boundary.

the control volume, T_{avg} can be considered as spatially uniform. Then the energy balance equation for the stationary control volume can be as following:

$$\frac{dT_{avg}}{dt} = \frac{d}{dt}\left(\frac{1}{x_e}\int_0^{x_e} T(x,t)dx\right) = \frac{1}{\rho_l c_{pl} x_e}\left[q_d(t) - q_c(t)\right] \tag{3.1}$$

where, ρ_l = density of liquid; c_{pl} = specific heat of the liquid.

3.3 Boiling Explosion Condition

The definition of explosive boiling adopted in this model implies a particular stage of the boiling process denoting massive scale vaporization rather than the initiation of the boiling process. Now, time dependent fluctuations of the average liquid temperature over the control volume, T_{avg}, occurs because of transient external energy deposition, q_d (t) and internal energy consumption due to bubble nucleation, q_c (t). According to Eq. (3.1), T_{avg}, will continue to increase until q_c (t) becomes equal to q_d (t) and at that moment, it reaches the maximum value, T^*_{avg}, at time, $t = t^*$. At the onset of this situation q_c $(t) \geq q_d$ (t) at $t = t^*$, the vapor generation continues on its own and an enormous amount of vapor prevents the liquid from contacting the solid by splashing the liquid away from the solid surface.

3.4 Energy Deposition in Liquid Cluster Due to External Heating

The rate of energy deposition in the liquid cluster (x_e) can be obtained from the difference in the heat fluxes across the cluster,

$$q_d(t) = -\lambda_l \left[\left.\frac{\partial T}{\partial x}\right|_{x=0} - \left.\frac{\partial T}{\partial x}\right|_{x=x_e} \right] \tag{3.2}$$

where, λ_l = thermal conductivity of liquid.

3.5 Energy Consumption in Liquid Cluster

By multiplying the size of liquid control volume (x_e) with the latent heat of vaporization (L) corresponding to the condition of homogeneous nucleation and the specific rate of vapor generation per unit mixture volume, $\Gamma_G(t)$, the rate of energy consumption in the liquid control volume due to boiling, $q_c(t)$, can bedetermined, as shown below :

$$q_c(t) = L\Gamma_G(t)x_e \tag{3.3}$$

Elias and Chambre [78], have defined the specific rate of vapor generation at any time, t, by the following integral as a function of the rate of homogeneous nucleation events (J), bubble radius transient r (t, t') and vapor density (ρ_v) as -

$$\Gamma_G(t) = \int_0^t \left\{ 4\pi r^2 \frac{dr(t,t')}{dt} \rho_v \right\} J(t') dt' \tag{3.4}$$

The specific rate of vapor generation per unit mixture volume, $\Gamma_G(t)$, relies heavily on rate of homogeneous nucleation events, J, which is the number of bubble nucleus formed during homogeneous boiling in unit time per unit volume. Carey [74] proposed the following relation for the rate of homogeneous nucleation events per unit liquid volume, J ($m^{-3}s^{-1}$), at any liquid temperature, T_l:

$$J(T_l) = 1.44 \times 10^{40} \sqrt{\frac{\rho_l^2 \sigma}{M^3}} \exp \left\{ \frac{1.213 \times 10^{24} \sigma^3}{T_l \{P_{ve}(T_l) - P_0\}^2} \right\} \tag{3.5}$$

where, J is in $m^{-3}s^{-1}$, P_{ve} and P_0 are in Pa, T_l is in K, σ is in N/m , ρ_l is in kg/m^3 and M is in kg/kg mol.

The variation of nucleation rate with liquid temperature for ethanol at atmospheric pressure is shown in Fig. 3.2

According to Skripov [26], the bubble radius transient, r (t), generated at time t' in a uniformly superheated liquid (T_l) as a function of time can be given as,

$$r(t,t') = \phi\sqrt{t - t'} \tag{3.6}$$

where

$$\phi = 2\sqrt{\frac{3}{\pi}} \frac{\sqrt{\lambda_l \rho_l c_l}}{L\rho_v} (T_l - T_s) \tag{3.7}$$

Where, T_s = saturation temperature at the bulk liquid pressure.
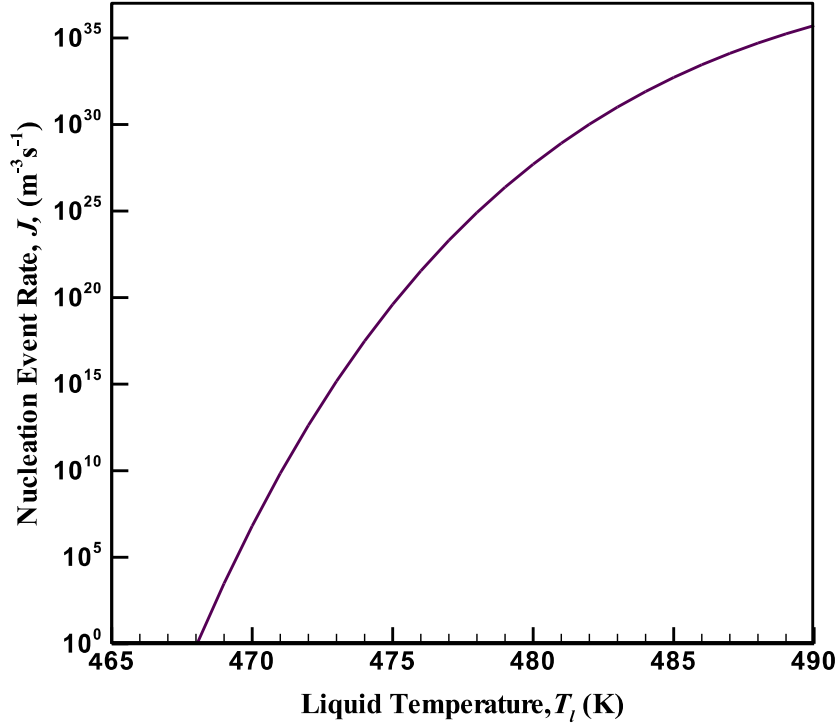
Fig. 3.2: Homogeneous nucleation rate, J on various liquid temperatures (T_l) for ethanol at atmospheric pressure

Upon substituting Eq. (3.7) in Eq. (3.4) and substituting T_l for T_{avg}, the expression for the instantaneous vapor generation rate per unit mixture volume, $\Gamma_G(t)$, can be obtained as a function of the average liquid temperature, T_{avg}, as follows:

$$\Gamma_G(t) = 2\pi \int_0^t J\left(T_{avg}\right) \phi^3\left(T_{avg}\right) \rho_v \sqrt{t - t'}\, dt' \tag{3.8}$$

Substituting Eq. (3.9) in Eq. (3.3) and performing further simplification, the following equation is obtained for the instantaneous rate of boiling heat consumption due to homogeneous nucleation boiling, $q_c(t)$:

$$q_c(t) = 2\pi L \phi^3\left(T_{avg}\right) \rho_v x_e \int_0^t J\left(T_{avg}\right) \sqrt{t - t'}\, dt' \tag{3.9}$$

39

3.6 Governing Equation

By incorporating the expressions of $q_d(t)$ and $q_c(t)$ in Eq. (3.1), the following integro-differential equation is obtained for the average liquid temperature, T_{avg}, over a finite liquid cluster of a characteristic size, x_e, with the consideration of simultaneous homogeneous nucleation boiling during rapid liquid heating.

$$\frac{dT_{avg}}{dt} = \frac{1}{\rho_l c_l x_e}\left[-\lambda_l\left\{\left.\frac{\partial T}{\partial x}\right|_{x=0} - \left.\frac{\partial T}{\partial x}\right|_{x=x_e}\right\} - 2\pi L\phi^3\left(T_{avg}\right)\rho_v x_e\int_0^t J\left(T_{avg}\right)\sqrt{t-t'}dt'\right] \quad (3.10)$$

The initial condition for Eq. (3.11) corresponds to $T_{avg} = T_0$ at $t = 0$.

3.7 Temperature Distributions

The terms in Eq. (3.11) rely heavily on temperature. Therefore, by combining temperature distributions for different boundary conditions with Eq. (3.11), explosive boiling phenomenon can be predicted. Temperature distributions for different boundary conditions are given below:

Table 3.1 Temperature distribution in the liquid for linear boundary heating

Boundary condition ($x = 0$)	Temperature distribution
$T = bt$	$T(x,t) = T_0 + 4bt\, i^2 erfc\left(x/\sqrt{4\alpha t}\right)$ (3.11) Where, $i^2 erfc\left(\dfrac{x}{\sqrt{4\alpha t}}\right) = \dfrac{1}{4}\left[erfc\left(\dfrac{x}{\sqrt{4\alpha t}}\right)\right] - 2\left(\dfrac{x}{\sqrt{4\alpha t}}\right)ierfc\left(\dfrac{x}{\sqrt{4\alpha t}}\right)$ $ierfc\left(\dfrac{x}{\sqrt{4\alpha t}}\right) = \dfrac{1}{\sqrt{\pi}}\exp\left(-\dfrac{x^2}{4\alpha t}\right) - \left(\dfrac{x}{\sqrt{4\alpha t}}\right)erfc\left(\dfrac{x}{\sqrt{4\alpha t}}\right)$

3.8 Characteristic Liquid Cluster Size

Liquid cluster size is a crucial issue as the liquid temperature field is transient and non-uniform. But, it is very difficult to measure experimentally the exact size of liquid control volume needed for the boiling explosion to occur and no information has been reported in the literature up to date. Therefore, two different theoretical cluster size scales have been adopted in the present study to investigate the effect of liquid cluster size on the prediction of homogeneous boiling explosion condition and hence to find out an appropriate size scale for the study of homogeneous nucleation phenomena under non-equilibrium heating. These size scales are as follows:

Table 3.2 Summary of Different Cluster Size Models considered in the present study

Cluster Size Model	Definition
Critical Vapor Embryo Model	$x_e = 2r_c(T^*_{avg})$
Thermal Penetration Depth Model	$x_e = \sqrt{\alpha t^*}$

(i)   *Size of critical vapor embryo at maximum cluster temperature*

In this size scale, the embryo size at the maximum attainable temperature in the liquid cluster, T^*_{avg}, is considered as the cluster size (x_e) i.e.,

$$x_e = 2r_c(T^*_{avg}) ,\qquad\qquad(3.12)$$

where r_c = *radius of critical vapor embryo*

Carey [74] proposed the following equation for r_c in a superheated liquid (T_l):

$$r_c(T_l) = \frac{2\sigma(T_l)}{P_s(T_l)\exp\left[\{P_o - P_s(T_l)\}/\rho_l RT_l\right] - P_o}\qquad(3.13)$$

The variation of the radius of critical vapor embryo, r_c, with the average liquid temperature, T_{avg}, has been shown in Fig. 3.3 for ethanol at atmospheric pressure.
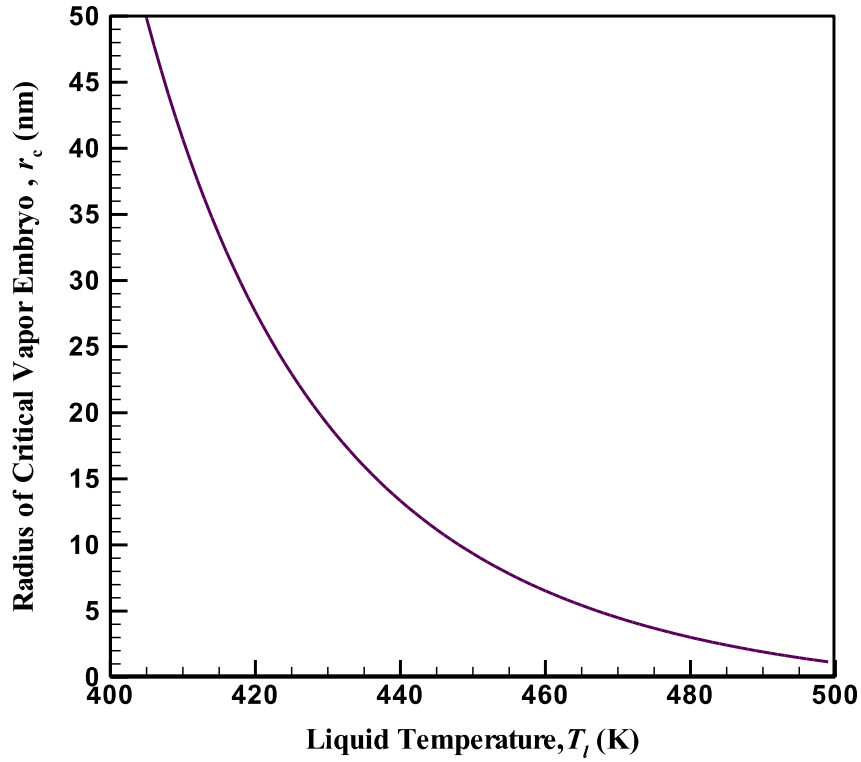
Fig. 3.3: Radius of the critical vapor embryo (r_c) on various liquid temperatures (T_l) for ethanol at atmospheric pressure.

(ii)   Thermal penetration depth

Thermal penetration depth is the thickness of the layer of liquid up to which heat can diffuse or penetrate through the liquid at a given time after the commencement of heating process.

According to this size scale, the cluster size, x_e, is equal to characteristic thermal penetration depth prior to the boiling explosion:

$$x_e = \delta_{th} = \sqrt{\alpha t^*} \tag{3.14}$$

where, α = thermal diffusivity of liquid; t^* = time of boiling explosion

The variation of penetration depth with the time of exposure for ethanol at atmospheric pressure is shown in Fig. 3.4.
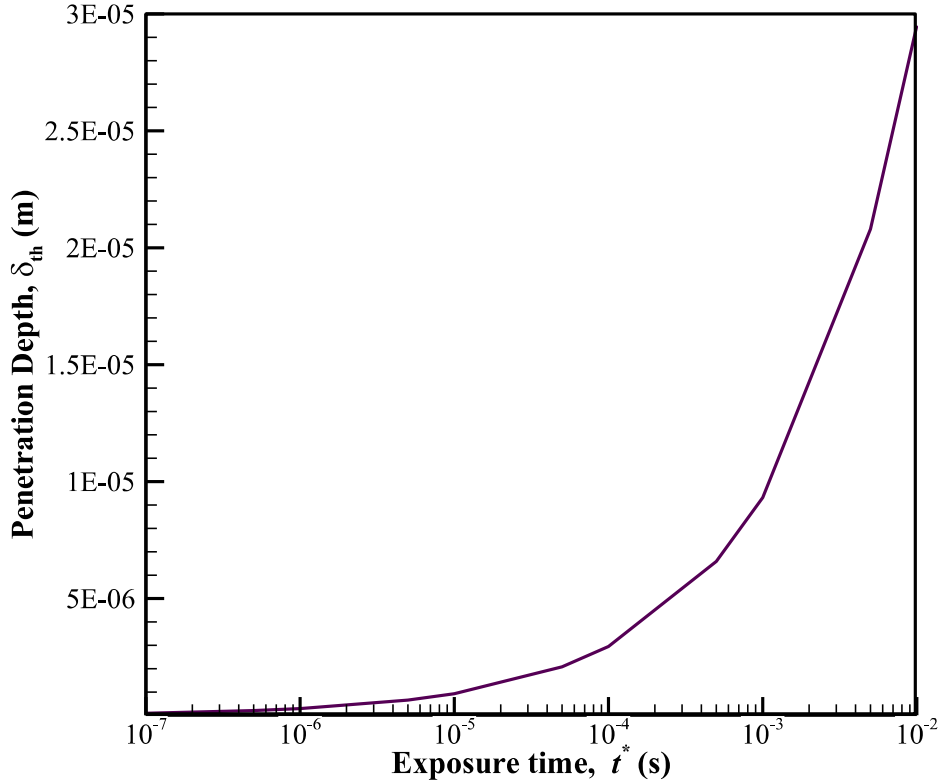
Fig. 3.4: Penetration depth at various exposure times for ethanol at atmospheric pressure.

3.9 Iteration Procedure and Calculation

At first, for average temperature, $T_{avg} = T_0$ at $t = 0$, an arbitrary value of thickness of the liquid control volume for instance, x_{ei} is assumed. For this, x_{ei}, the time-dependent fluctuations of T_{avg}, is then obtained by calculating the instantaneous energy deposition rate, $q_d(t)$ and energy consumption rate due to boiling, $q_c(t)$ in the liquid control volume as per Eq. (3.2) and Eq. (3.10). At $t = t^*$, $q_c(t)$ becomes equal to $q_d(t)$ with the maximum attainable liquid temperature in the cluster, $T_{avg} = T^*_{avg}$. This particular stage of bubble generation and growth has been defined as the boiling explosion condition. The maximum attainable temperature in the liquid cluster, T^*_{avg}, obtained for x_{ei} is then used to calculate the liquid control volume thickness or cluster size, x_e, as per Eq. (3.14) or Eq. (3.17) for the next iteration. This iteration procedure is repeated until it converges, that is, the absolute value of $(x_e - x_{ei})/x_{ei}$ becomes less than 0.0001. Finally, the temperature rise in the liquid control volume is obtained for the control volume thickness, x_e, and the boiling explosion characteristics such as liquid temperature limit (T^*_{avg}), time (t^*) at the

43

boiling explosion ($q_c(t) = q_d(t)$ and $dT_{avg}/dt = 0$) are determined. Note that, for temperature dependent vapor generation term, Γ_G (t) and other necessary thermodynamic properties of ethanol, the PROPATH software package developed by PROPATH GROUP [89] have been used.

3.10 Summary

A theoretical model [79] to study the process of explosive boiling has been described in this chapter. Energy balance equation inside a liquid cluster has been set. Boiling explosion in a liquid cluster is assumed to occur at a moment when energy consumed due to bubble generation and growth exceeds external energy deposition causing the liquid sensible energy to decrease i.e. $dT_{avg}/dt = 0$. Two different size scales for liquid cluster has been considered. All necessary equations to obtain the closed form solution of the given problem have been fixed with appropriate assumptions.

CHAPTER 4

RESULT AND DISCUSSION

4.1 Introduction

In the previous chapter, the macroscopic model for explosive boiling under non-equilibrium condition has been discussed. In this chapter, the model predicted results have been compared with experimental observations [31] for both characteristic liquid cluster size scales. Based on the comparison, a suitable size scale is chosen. Then for a particular initial temperature and different heating rate (10 -10^9 K/s), predicted boiling explosion conditions are compared with the theoretical explosion condition as given by Gambill and Lienhard [80] and the experimental observations noted by Avedisian [81]. Also the explosive boiling condition has been investigated from energy point of view and a novel criterion for explosive boiling has been found.

4.2 Model Prediction and Experimental Observation of Boiling Explosion

For the purpose of determining proper size scale for explosive boiling phenomenon analysis, comparison with experimental results is required. In the *Fig. 4.1-4.4* below, the experimental observations of micro scale boiling explosion in ethanol heating at atmospheric pressure reported by Okuyama et al. [31] have been shown. In addition, the time of boiling explosion as predicted by the model for two different cluster sizes has been mentioned in each case. In Table-4.1, the characteristics of explosive boiling for two different cluster sizes have been presented for various initial and boundary conditions identical to those of Okuyama et al. [31]. It is quite evident from the tables below each figure that, when critical vapor embryo ($x_e = 2r_c(T^*_{avg})$) at maximum cluster temperature (T^*_{avg}) is considered as cluster size, the time of boiling explosion, t^* obtained from the model are in reasonable agreement with the experimental observation in all cases. But for liquid cluster size equal to thermal penetration depth ($x_e = \sqrt{\alpha t^*}$), t^* lags far behind the experimental observation for all cases. But for both cluster size model, predicted temperature limit at the boiling explosion is very close which suggests that explosive boiling phenomenon is governed by the liquid temperature.

46
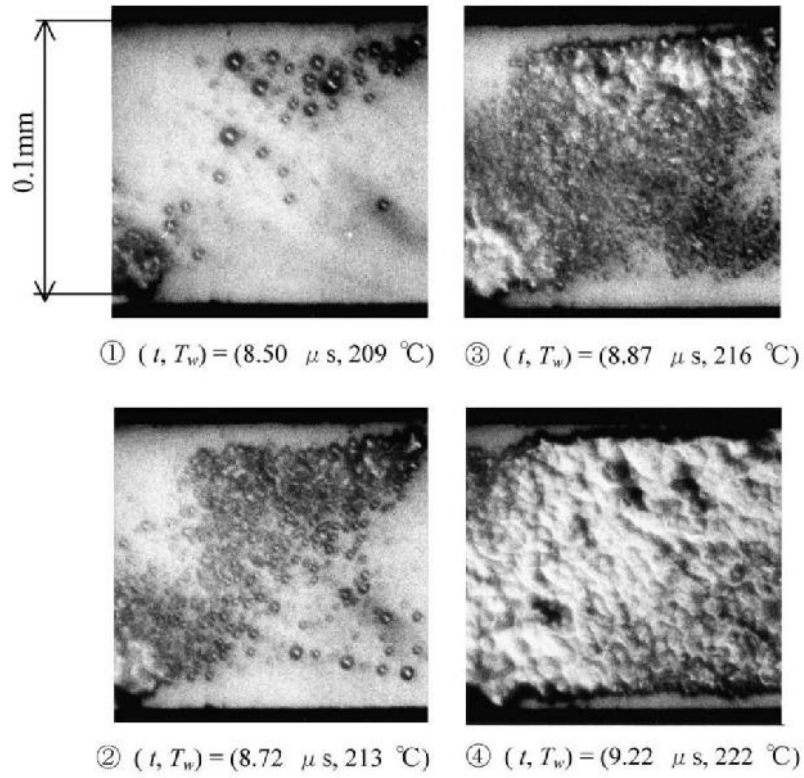
Fig. 4.1: Magnified top view of boiling bubbles immediately after boiling incipience on the film heater subjected to high pulse heating. (ethyl alcohol, P = 0.1MPa, T_0= 25^{0}C, b = 2.2×10^7 K/s)[31]

Model Prediction:

Cluster Size Model	Time of Boiling Explosion, t^*(s) $(\frac{\delta T_{avg}}{\delta t} = 0, \frac{\delta^2 T_{avg}}{\delta t^2} < 0)$
$x_e = 2r_c(T^*_{avg})$	8.12×10^{-06}
$x_e = \sqrt{\alpha t^*}$	13.94×10^{-06}
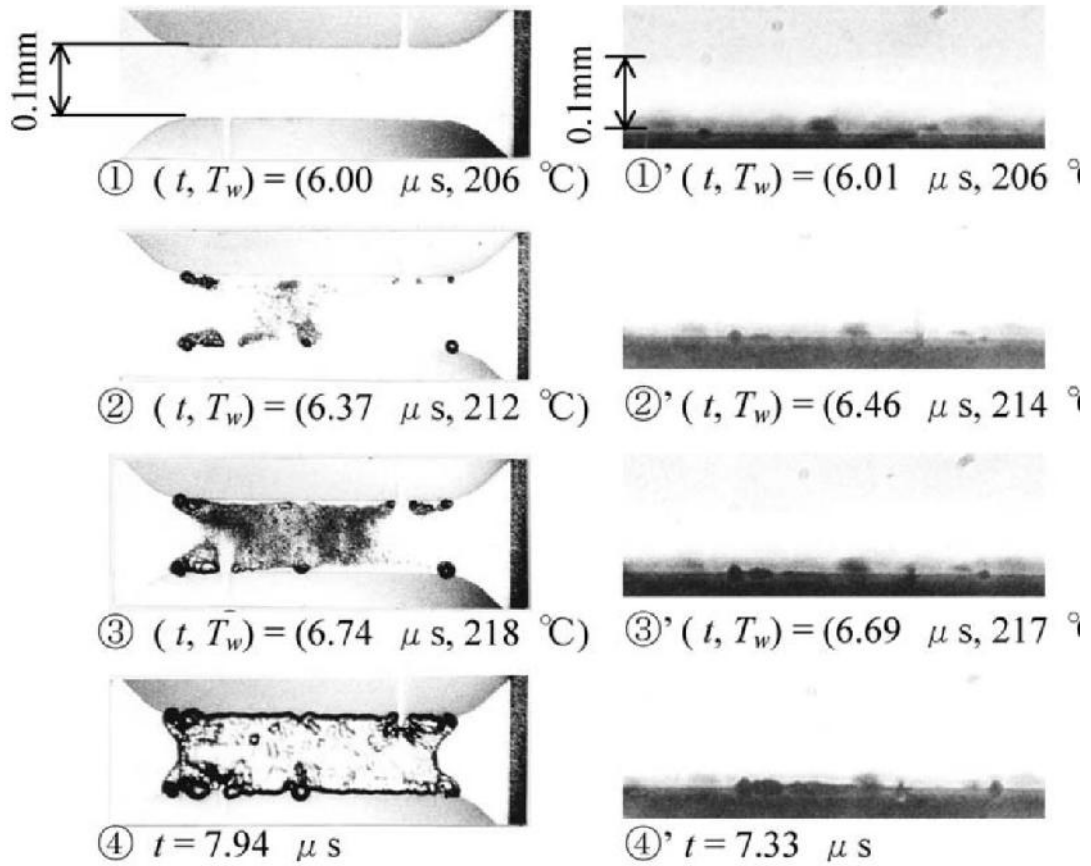
Fig. 4.2: Top and side views of boiling bubbles after boiling incipience on the film heater subjected to high pulse heating. (ethyl alcohol, P = 0.1MPa, T_0=25^0 C, b = 3.0×10^7 K/s,)[31]

Model Prediction:

Cluster Size Model	Time of Boiling Explosion, t^*(s) $(\frac{\delta T_{avg}}{\delta t} = 0, \frac{\delta^2 T_{avg}}{\delta t^2} < 0)$
$x_e = 2r_c(T^*_{avg})$	5.97 × 10^{-06}
$x_e = \sqrt{\alpha t^*}$	10.24 × 10^{-06}
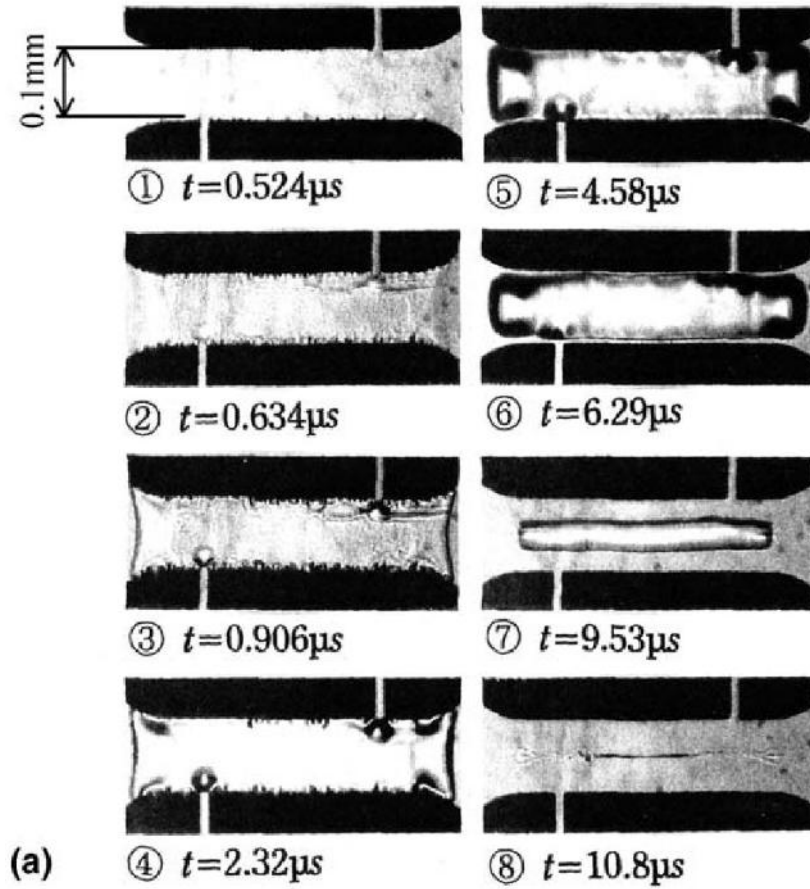
Fig. 4.3: Boiling configurations after boiling incipience on the film heater at high heating rates. (ethyl alcohol, P = 0.1MPa, T_0=25^0 C, b = 3.7×10^8 K/s)[31]

Model Prediction:

Cluster Size Model	Time of Boiling Explosion, t^*(s) $(\dfrac{\delta T_{avg}}{\delta t} = 0, \dfrac{\delta^2 T_{avg}}{\delta t^2} < 0)$
$x_e = 2r_c(T^*_{avg})$	0.49×10^{-06}
$x_e = \sqrt{\alpha t^*}$	0.84×10^{-06}
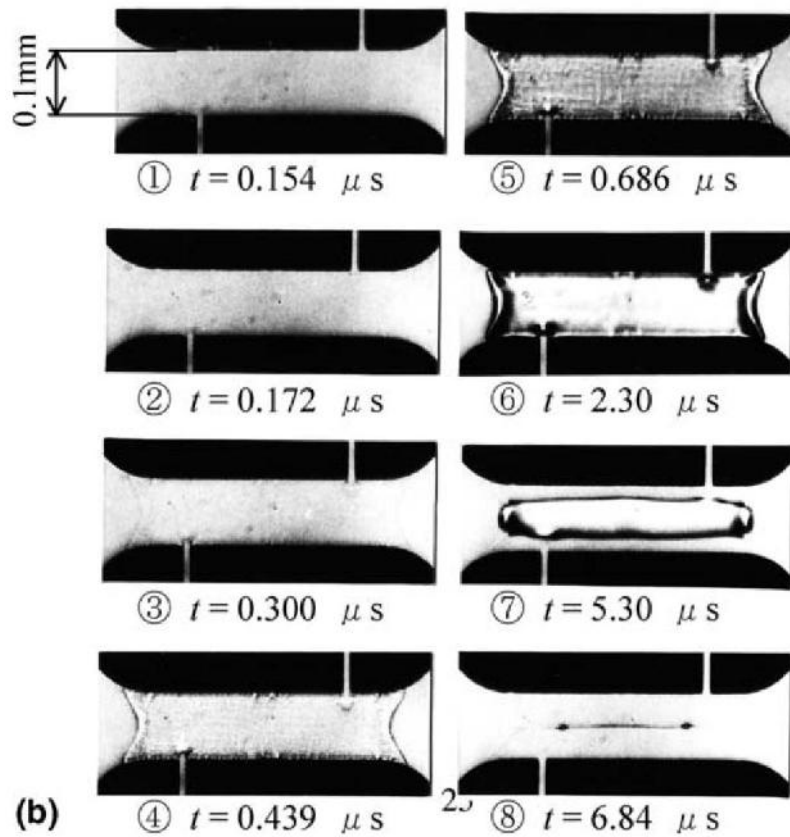
Fig. 4.4: Boiling configurations after boiling incipience on the film heater at high heating rates. (Ethyl alcohol, P = 0.1MPa, $T_0=25^0$ C, b = 1.2×10^9 K/s)[31]

Model Prediction:

Cluster Size Model	Time of Boiling Explosion, t^*(s) $(\dfrac{\delta T_{avg}}{\delta t} = 0, \dfrac{\delta^2 T_{avg}}{\delta t^2} < 0)$
$x_e = 2r_c(T^*_{avg})$	0.16×10^{-06}
$x_e = \sqrt{\alpha t^*}$	0.26×10^{-06}

Table- 4.1: Comparison of Simulation Result for Different Characteristic Cluster Size (x_e)

Heating Rate, b (K/s)	Cluster Size Model					
	$x_e = 2r_c(T^*_{avg})$			$x_e = \sqrt{\alpha t^*}$		
	x_e(m)	t^*(s)	T^*_{avg}(K)	x_e(m)	t^*(s)	T^*_{avg}(K)
2.2×10^7	7.20×10^{-09}	8.12×10^{-06}	475.66	1.10×10^{-06}	13.94×10^{-06}	475.62
3.0×10^7	7.13×10^{-09}	5.97×10^{-06}	475.90	0.94×10^{-06}	10.24×10^{-06}	475.86
3.7×10^8	6.70×10^{-09}	0.49×10^{-06}	477.43	0.27×10^{-06}	0.84×10^{-06}	477.39
1.2×10^9	6.52×10^{-09}	0.16×10^{-06}	478.08	0.15×10^{-06}	0.26×10^{-06}	477.86

From the simulated result above, it can be seen that, with liquid cluster considered as the critical vapor embryo, the boiling explosion timepredicted by the model are in good agreement with experimental result. But when thermal penetration depth is considered as liquid cluster, the model predicted time for boiling explosion differs a lot with the experimental result. Also the cluster size in these two models differs roughly by three orders of magnitude. Therefore, it is clear that a liquid cluster equal to the size of a critical vapor embryo at maximum cluster temperature corresponds to a suitable length scale for homogeneous boiling study during non-equilibrium heating. Therefore, this cluster size is selected for theoretical prediction of homogeneous boiling characteristics for ethanol heating at atmospheric pressure over a wide range of heating ($10 - 10^9$ K/s) which incorporates different liquid heating technique such as bubble column, droplet superheating , pulse heating etc.

4.3 Explosive Boiling Characteristics at Different Boundary Heating Rates

Considering critical vapor embryo at maximum temperature as the liquid cluster, explosive boiling phenomenon has been simulated for various heating rates at an initial temperature of 25^0C.

In *Fig. 4.5,* the temperature escalation inside the liquid cluster during heating of ethanol at various boundary heating rates. It can be seen that, with the increase of boundary heating rate, the explosive boiling condition is achieved in lesser time and at higher temperature with deeper penetration into the metastable liquid state.

In *Fig. 4.6,* the effects of boundary heating rate on time and temperature of boiling explosion is shown. The degree of variation in the time of boiling explosion with increasing boundary heating

rate is drastic; almost of inverse order of heating rate.But the maximum cluster temperature varies about 9°C over the entire range of heating rate.These maximum cluster temperature obtained for various boundary heating rates are very close to the superheat limit of ethanol as mentioned by Avedisian [81]. The nucleation event rate corresponding to the maximum cluster temperature, obtained from the model, varies from 10^{11} to $10^{24} \mathrm{m}^{-3}\mathrm{s}^{-1}$. This is in good agreement with the approximate nucleation rates found in various experimental observations noted by Avedisian [81].

Table- 4.2: Typical Nucleation Rates Obtained with different Superheat-Measuring Technique [81]

Liquid Heating Method	Nucleation Event Rate, J ($\mathrm{m}^{-3}\mathrm{s}^{-1}$)
Bubble Chamber	10^{8} to 10^{11}
Capillary Tube	10^{11} to 10^{11}
Droplet Superheat	10^{12} to 10^{13}
Pulse Heating	10^{21} to 10^{28}

Table- 4.3: Summary of the Simulated Result for Characteristic Cluster Size ($x_e = 2r_c(T^*_{avg})$)

b (K/s)	x_e(nm)	t* (s)	T^*_{avg} (K)
10	9.11	17.165	469.65
10^3	8.57	0.1732	471.24
10^5	7.98	1.752×10^{-3}	473.08
10^6	7.65	1.763×10^{-4}	474.12
10^7	7.32	1.78×10^{-5}	475.27
10^8	6.95	1.8×10^{-6}	476.54
10^9	6.55	1.85×10^{-7}	477.97
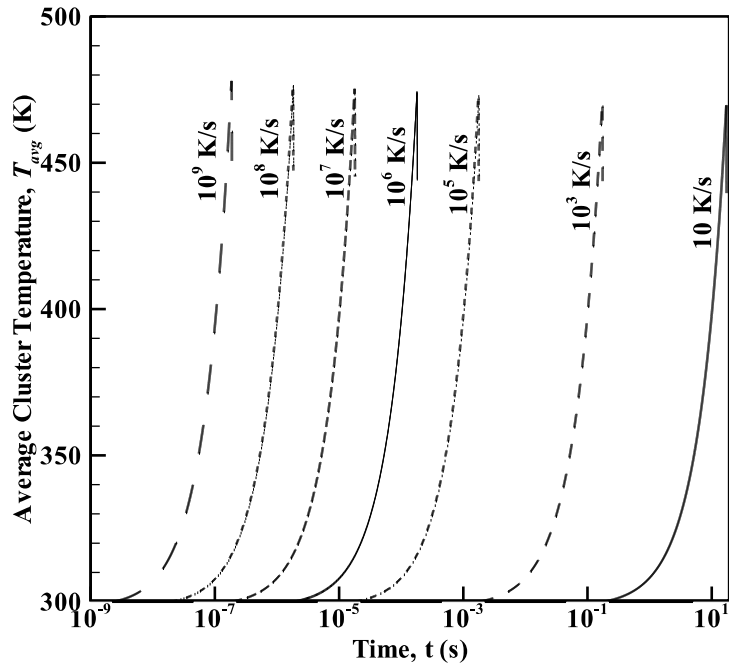
Fig. 4.5: Temperature escalation inside the liquid cluster at various boundary heating rates.
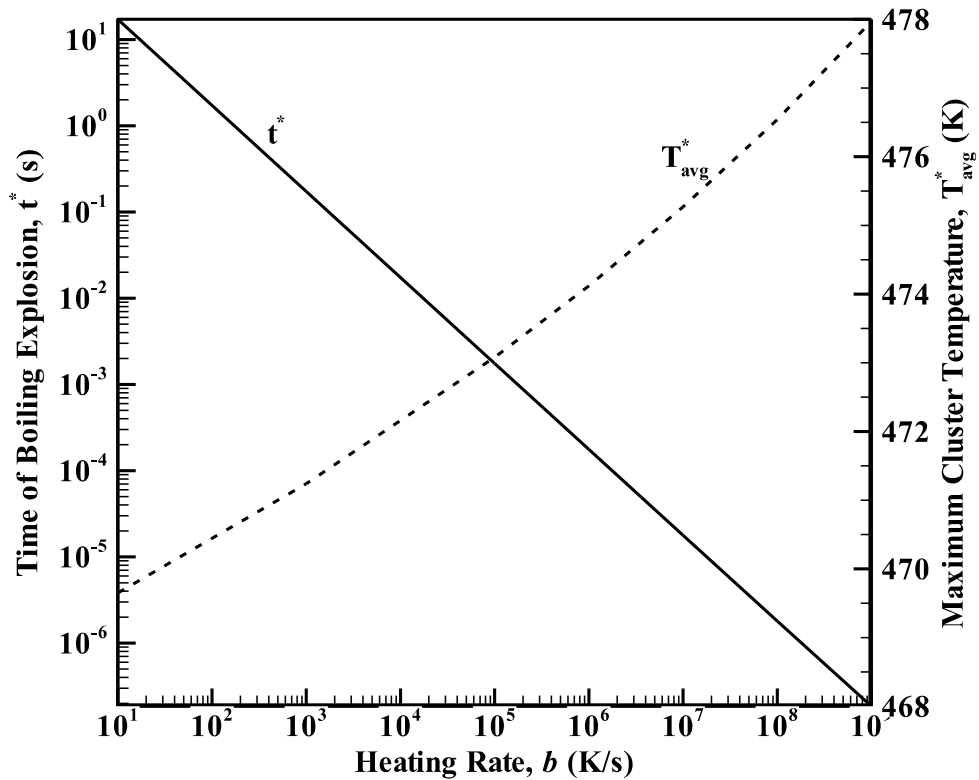
Fig. 4.6: Effect of boundary heating rate (b) on the time and temperature of homogeneous boiling explosion or explosive boiling.

4.4 Heat Flux Characteristics at Liquid-Vapor Interface during Explosive Boiling

The explosive boiling condition predicted by the macroscopic model can be compared with the theoretical explosion condition obtained in terms of maximum possible heat flux across the liquid-vapor interface, $q_{max,max}$. The expression of maximum possible heat flux across the liquid-vapor interface, $q_{max,max}$, that can be achieved in a vaporization or condensation process, as proposed by Gambill and Lienhard [80] , is as follows,

$$q_{\max,\max} = \rho_v L \sqrt{RT / 2\pi} \tag{4.1}$$

where, L = Latent heat of vaporization; ρ_v = Vapor density; R = Universal gas constant

Now, the heat flux across liquid-vapor interface of a vapor bubble at time of explosive boiling, t^*, q_{l-v} is expressed as,

$$q^*{}_{l-v} = \rho_v L \left. \frac{dr}{dt} \right|_{t=t^*} \tag{4.2}$$

But at $t = t^*$, vapor bubbles of different sizes co-exist. This means the individual bubble has its own growth rate depending on its lifetime that is; it grows at the different heat flux across the liquid vapor interface. Therefore, the largest heat flux at the interface is chosen which is generated just before the boiling explosion. Near the time of explosion, the growth of the bubble is controlled by the inertia. To calculate the maximum bubble heat flux, $q^*{}_{l-v}$, considering inertia controlled bubble growth; the bubble growth model proposed by Rayleigh [82] is used.

Summarization of maximum heat flux across the liquid-vapor interface at the boiling explosion, $q^*{}_{l-v}$, and corresponding upper limit of evaporative heat flux, $q_{max,max}$, obtained from model is given below:

Table- 4.4: Summary of the Simulated Result for $q^{*}_{l\text{-}v}$ and $q_{max,max}$

b (K/s)	x_e (nm)	t^{*} (s)	T^{*}_{avg}(K)	$q^{*}_{l\text{-}v}$ (W/m^2)	$q_{max,max}$ (W/m^2)
10	9.11	17.165	469.65	1.35×10^{9}	2.77×10^{9}
10^{3}	8.57	0.1732	471.24	1.4×10^{9}	2.84×10^{9}
10^{5}	7.98	1.752×10^{-3}	473.08	1.47×10^{9}	2.92×10^{9}
10^{6}	7.65	1.763×10^{-4}	474.12	1.51×10^{9}	3.97×10^{9}
10^{7}	7.32	1.78×10^{-5}	475.27	1.56×10^{9}	3.02×10^{9}
10^{8}	6.95	1.8×10^{-6}	476.54	1.61×10^{9}	3.07×10^{9}
10^{9}	6.55	1.85×10^{-7}	477.97	1.67×10^{9}	3.14×10^{9}

From the above table, it can be seen that for all cases, $q^{*}_{l\text{-}v}$ is lower than $q_{max,max}$. The reason is that, for obtaining $q_{max,max}$, assumption of no condensation at the liquid-vapor interface has been made. But in reality there must be some condensation in parallel with vaporization. Therefore, the obtained results are in agreement with theoretical explosion condition.
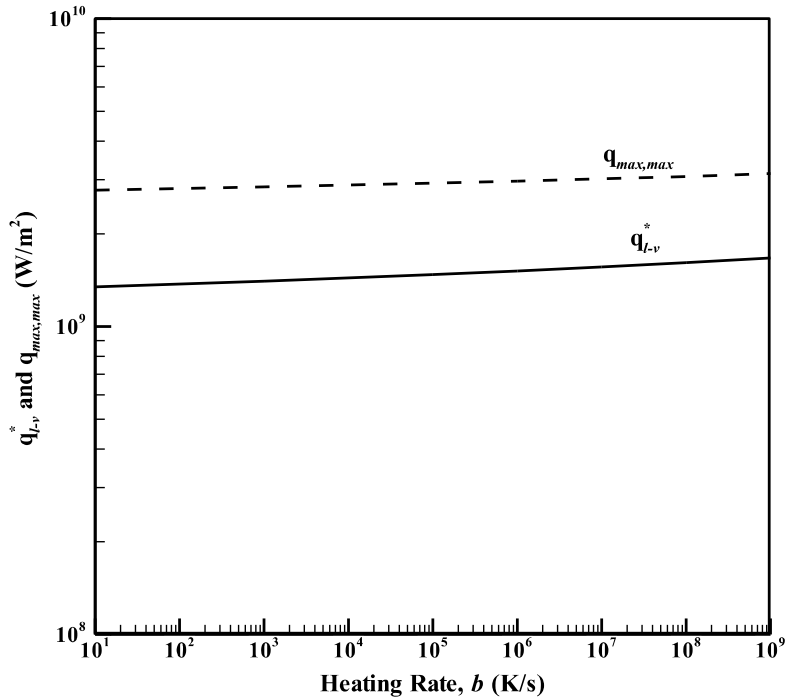
Fig. 4.7: Variation of heat flux across liquid-vapor interface of a vapor bubble at time of explosive boiling, t^{*}, $q_{l\text{-}v}$ and maximum possible heat flux across the liquid-vapor interface, $q_{max,max}$ with Boundary Heating Rate.

4.5 Continuum Characteristics of Liquid Cluster

The macroscopic model used in this study stands on continuum condition. As mentioned by Gad-el-Hak [83], continuum consideration may be applicable for liquid thickness over 10 molecular layers. For vapor bubbles, the number of molecules in the critical bubble at the boiling explosion has been considered as the continuum characteristic. From the Table- 4.3, it can be seen that, the size of the critical cluster (x_e) decreases as the boundary heating rate, b, increases. However, with the presence of 15 bubbles in critical cluster (diameter of ethanol = 0.44 nm) for the smallest cluster size in Table- 4.3, it can be assumed that, continuum condition is achieved.

4.6 Effect of Liquid Sub-cooling

In the present study, the time of boiling explosion, t^*, has been determined for different heating rate (10K/s-10^9 K/s) for a range of initial liquid temperature , T_0 (25^0C – 78^0C). These results have been tabulated below.

Table- 4.5: Time of Boiling Explosion for Various Liquid Initial Temperatures

b (K/s)	x_e (nm)	t^* (s)		
		$T_0 = 25^0C$	$T_0 = 50^0C$	$T_0 = 78^0C$
10	9.1126	17.165	14.665	11.834
10^3	8.5723	0.17326	0.14826	0.11996
10^5	7.9789	1.7519×10^{-3}	1.5018×10^{-3}	1.2188×10^{-3}
10^6	7.6572	1.7638×10^{-4}	1.5136×10^{-4}	1.2305×10^{-4}
10^7	7.3154	1.7794×10^{-5}	1.5290×10^{-5}	1.2455×10^{-5}
10^8	6.9499	1.8043×10^{-6}	1.553×10^{-6}	1.2684×10^{-6}
10^9	6.557	1.8544×10^{-7}	1.6005×10^{-7}	1.3128×10^{-7}

From the above table, it can be understood that, for a particular boundary heating rate, t^* depends on T_0, as the nucleation occurs earlier for a higher liquid initial temperature. However, as the nucleation occurs at a much higher temperature range than liquid initial temperature, no substantial effect of T_0 on T^*_{avg} has been found. Therefore, T^*_{avg} depends only on the liquid heating rate, b, as reported in Hasan and Monde[84].

For the ethanol heating at atmospheric pressure, the macroscopic model used here, proposes the following approximate equations for the time of boiling explosion, $t^*(\mu s)$, and the maximum attainable liquid temperature, $T^*_{avg}(K)$, for a wide range of boundary heating rate, b, and liquid initial temperature, $T_0(K)$, as,

$$t^* = \left[1.94 - 0.01 \times (T_0 - 273)\right] \times 10^8 \times b^{-0.995} \tag{4.3}$$

$$T^*_{avg} = 0.45 \ln(b) + 468.2 \tag{4.4}$$

For $10 < b < 10^9$ K/s and $298 < T_0 < 351$ K.
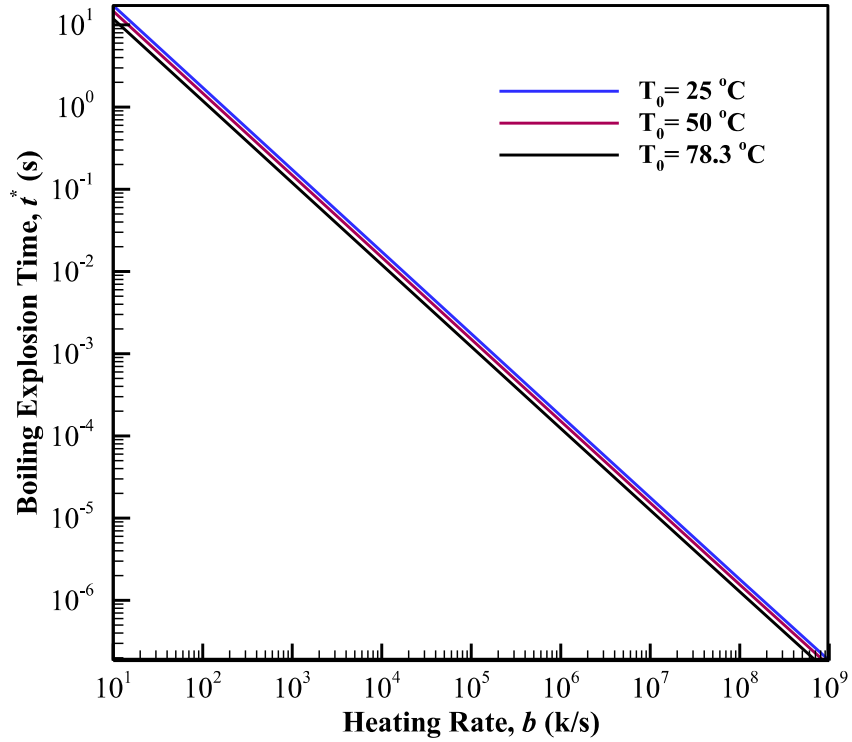
Fig. 4.8: Variation of boiling explosion time , t^*,at liquid initial temperatures 25^0, 50^0 and 78.3^0C.

4.7 Comparison of the Present Results with other Theoretical Prediction

The results regarding the occurrence of explosive boiling obtained from the present model (which is essentially a macroscopic model based on bubble generation and growth) can be compared with other model's prediction that are based on other theoretical approaches such as atomic or pseudo-atomic models. As an example, we may consider the pseudo-atomic model

reported by Lu and Ding [85]. In their model [85], they considered the long-range inter molecular forces near the solid heater wall that essentially affect the liquid adjacent to the wall and associated boiling phenomena. Using the Hamaker constant (A_{slv}) and the interaction potential between the wall and the liquid, they obtained the thickness of stable liquid layer (h_c) over the solid wall as a function of the wall temperature (T_w) as follows:

$$h_c = \sqrt{\frac{A_{slv}}{6\pi[P_s(T_w) - P_0]}} \qquad (4.5)$$

For ethanol heating at atmospheric pressure, the variation of the thickness of stable liquid layer (h_c) with wall temperature (T_w) is shown in Fig. 4.9. For comparison, the variation of the size of critical vapor embryo ($x_e = 2r_c$) which has been considered as the size scale in the present model has also been depicted in Fig. 4.9. Noteworthy that, the size scale considered in the present model (x_e) is much greater than the thickness of stable liquid layer (h_c) for any wall temperature (T_w). Therefore, it can be assumed that sufficient number of liquid atoms can reside inside the liquid cluster to instigate the boiling phenomena.
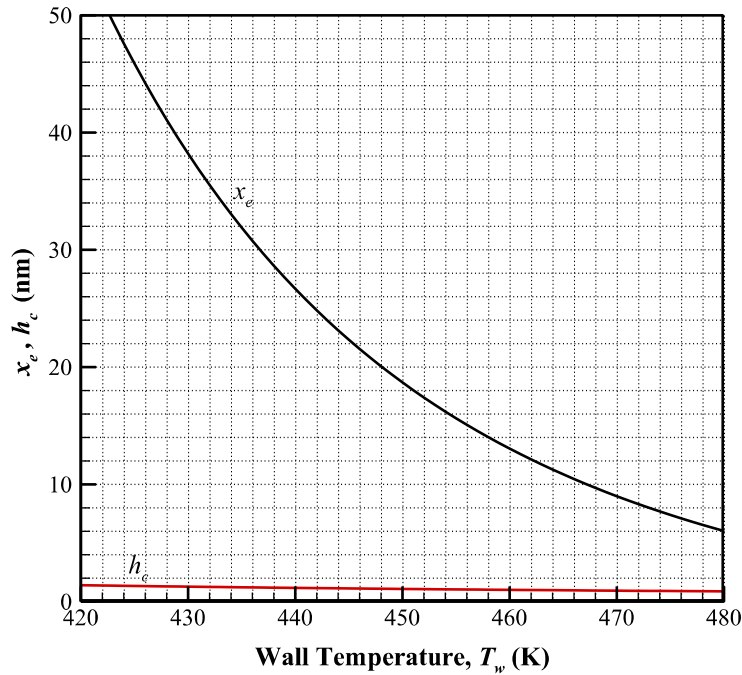
Fig. 4.9: Variation of the size of critical vapor embryo and thickness of stable liquid layer [85] with wall temperature for ethanol at atmospheric pressure

58

Apart from the size consideration of the present model, let us focus on the time of boiling explosion as predicted in the present model. In the pseudo-atomic model of Lu and Ding [85], the minimum time required for boiling explosion has been anticipated at a condition when the wall temperature becomes equal to a special temperature, T_t such that:

$$t^*_{min} \geq \frac{(T_t - T_0)}{b} \tag{4.6}$$

The special temperature, T_t considered by Lu and Ding [85] corresponds to value at which the radius of critical vapor embryo (r_c) equals to critical distance of maximum supersaturation, h_p. The critical distance of maximum supersaturation, h_p, as defined by Lu and Ding [85] depends on molecular interaction (A_{slv}), wall temperature (T_w), liquid spatial temperature gradient, (β) as well as equilibrium thermodynamic properties (specific volume, v and latent heat of vaporization h_{lv}) as given below:

$$h_p = \sqrt[4]{\frac{A_{slv} T_w \Delta v}{2\pi\beta h_{lv}}} \tag{4.7}$$

For the case of linear heating at the boundary ($T_w = bt$ at $x = 0$), liquid spatial temperature gradient (β) near the boundary can be obtained as:

$$\beta = \frac{dT}{dx} \approx b\sqrt{\frac{t}{4\alpha}} \tag{4.8}$$

The variation of h_p and r_c along with the wall temperature, T_w are shown in Fig. 4.10 for different boundary heating rates (b). From Fig. 4.10, it is evident that the value of T_t (the temperature at which $r_c = h_p$) depends on the rate of boundary heating rate. As the boundary heating rate increases, T_t also increases.
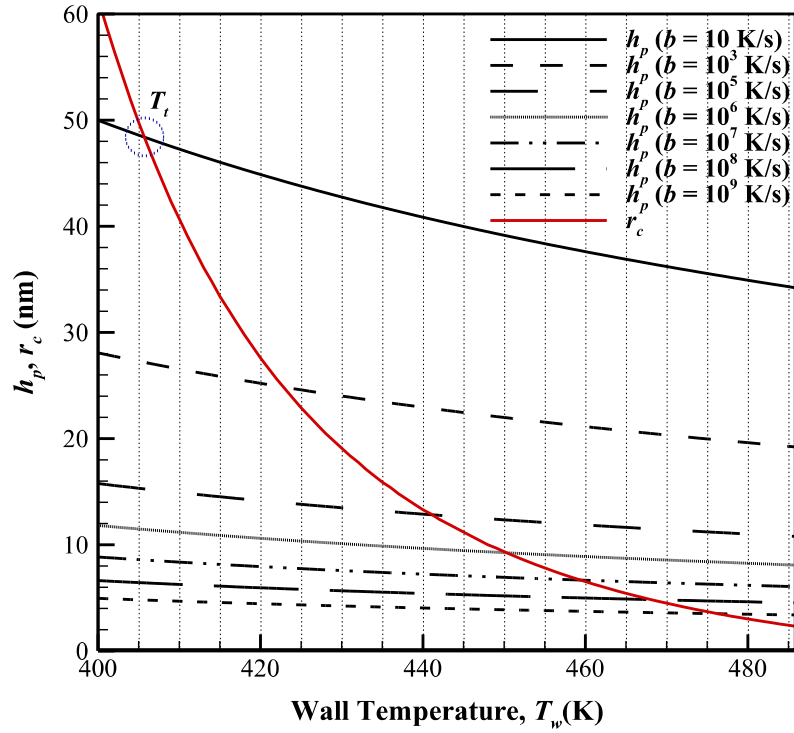
Fig. 4.10: Critical bubble radius (r_c) and critical supersaturation distance (h_p) for ethanol at various boundary heating rates

The comparison of the results obtained in the present study and that obtained by following the model presented Lu and Ding [85] has been summarized in Table 4.6. As mentioned there, the time of boiling explosion as predicted by the present model satisfies the condition that is the minimum time required for the explosive boiling as described by Eq. 4.6.

Table- 4.6: Comparison of time of boiling explosion time predicted by present model and that Lu and Ding [85]

b (K/s)	t^* (s) $q_c(t) \geq q_d(t)$	t^*_{min} (s)[85] $t^*_{min} \geq \dfrac{(T_t - T_0)}{b}$
10	17.165	10.701
10^3	0.1732	0.125
10^5	1.752×10^{-3}	1.42×10^{-3}
10^6	1.763×10^{-4}	1.53×10^{-4}
10^7	1.78×10^{-5}	1.62×10^{-5}
10^8	1.8×10^{-6}	1.7×10^{-6}
10^9	1.85×10^{-7}	1.78×10^{-7}

4.8 Explosive Boiling From an Energy Point of View

Applying the macroscopic model for boiling explosion, explosive boiling characteristics that is; time of boiling explosion, t^*, characteristic liquid cluster size, x_e, and maximum attainable temperature, T^*_{avg} , can be determined for any liquid. Hasan et al. [79, 86-87] have determined explosive boiling characteristics for water at initial temperature (T_0) of 20^0C for three types of boundary heating condition. These conditions are:

i) Linear Boundary Heating *(T = bt; 10 < b <10^9 K/s)*

ii) High Heat Flux Boundary Condition *(q = q$_w$; 15 <q$_w$< 1000 MW/m^2)*

iii) Constant Temperature Boundary Condition *(T = T$_i$; 303 < T$_i$< 307 ^{0}C)*

The summary of explosive boiling characteristics obtained from the model for these boundary conditions are given below:

Table-4.7: Homogeneous nucleation boiling characteristics during linear boundary heating of water (20 °C) [79]

$b(K/s)$	$x_e(nm)$	$T^*_{avg}(°C)$	$t^*(s)$
10	6.72	301.8	2.82×10^1
10^3	6.32	303.9	2.84×10^{-1}
10^5	5.88	306.3	2.87×10^{-3}
10^7	5.38	309.2	2.90×10^{-5}
10^9	4.79	312.8	2.97×10^{-7}

Table-4.8: Homogeneous nucleation characteristics during high heat flux (q) pulse heating of water (20°C) [86]

$q_w(W/m^2)$	$x_e(nm)$	$T^*_{avg}(°C)$	$t^*(s)$
15×10^6	5.81	306.7	7.23×10^{-4}
100×10^6	5.39	309.1	16.547×10^{-6}
250×10^6	5.17	310.4	2.684×10^{-6}
500×10^6	5.00	311.5	6.808×10^{-7}
750×10^6	4.89	312.2	3.0601×10^{-7}
1000×10^6	4.81	312.7	1.7386×10^{-7}

Table- 4.9: Homogeneous nucleation boiling characteristics during water (20 °C) contact with

hot carbon steel surface (β = 8.81) [87]

$T_b(°C)$	$T_i(°C)$	$x_e(nm)$	$T^*_{avg}(°C)$	$t^*(s)$
336	303.9	6.41	303.4	$4.4346×10^{-4}$
337	304.8	6.26	304.2	$1.1742×10^{-4}$
338	305.7	6.12	305.0	$0.3611×10^{-4}$
339	306.6	5.99	305.7	$0.1285×10^{-4}$
340	307.5	5.87	306.3	$0.5239×10^{-5}$

From Tables- 4.7-4.9, it is clear that both time and temperature at the boiling explosion change with the heating parameter especially the variation of time is very drastic. But for a specific liquid initial condition, explosive boiling condition should remain a unique state regardless of heating parameter and method. Therefore, the aim of the present study is to find out a unique criterion for homogeneous boiling explosion or explosive boiling from an energy point of view.

4.9 Formulation of Cumulative Energy Density in the Liquid at Explosive Boiling Condition

For simplification, the temperature distribution, which is the distribution of energy added to the liquid at any instance of time, is presented in terms of non-dimensional temperature, θ and modified Fourier Number, η for various boundary conditions at $x = 0$.

The modified Fourier number is defined as:

$$\eta = \frac{x}{\sqrt{4\alpha t}}$$

(4.9)

While the expression of θ varied for each boundary condition.

The temperature distributions for three different boundary conditions are given below:

Case 1: For linearly increasing temperature boundary condition ($T = bt$):

$$T(x,t) = T_0 + 4bti^2 erfc(x/\sqrt{4at})$$
(4.10)

$$\theta = \frac{T(x,t) - T_0}{bt} = 4i^2 erfc(\eta)$$
(4.10a)

where, b = Boundary Heating Rate. (K/s)

Case 2: For constant heat flux boundary condition ($q = q_w$):

$$T(x,t) = T_0 + \frac{q_w \sqrt{\alpha t}}{\lambda} erfc(x/\sqrt{4at})$$
(4.11)

$$\theta = \frac{T(x,t) - T_0}{q_w \sqrt{\alpha t}/\lambda} = 2ierfc(\eta)$$
(4.11a)

where, q_w = Boundary Heat Flux. (W/m^2)

Case 3: For constant temperature boundary condition ($T = T_i$):

$$T(x,t) = T_0 + (T_i - T_0) erfc(x/\sqrt{4at}); \quad T_i = (\beta T_b + T_0)/(1 + \beta)$$
(4.12)

$$\theta = \frac{T(x,t) - T_0}{T_i - T_0} = erfc(\eta)$$
(4.12a)

where, T_i = Solid-Liquid Interface Temperature. (^{0}C)

For clearer visualization of accumulated energy distribution inside the liquid during heat process, the percentage of cumulative energy $E(\eta)$ residing within the range $0-\eta$ to the total energy deposited $E(\infty)$ in the liquid $(0-\infty)$ at any instant of time as defined below:

$$\% \ of \ total \ accumulated \ energy = \frac{E(\eta)}{E(\infty)} \times 100\% = \frac{\int_0^\eta \theta(\eta)d\eta}{\int_0^\infty \theta(\eta)d\eta} \times 100\%$$
(4.13)

For any value of η, average cumulative energy density (energy per unit liquid volume) is defined as below:

$$\dot{E}(\eta) = \frac{E(\eta)}{\eta} = \frac{\int_0^\eta \theta(\eta) d\eta}{\eta}$$

(4.14)

If the cumulative energy density corresponding to the thermal penetration depth (δ_{th}) is considered as reference, the relative energy density factor for any value of η will be as follows:

$$m = \frac{\dot{E}(\eta)}{\dot{E}(\delta_{th})} = \frac{E/\eta}{E/\delta_{th}}$$

(4.15)

Once the relative energy density factor, m, corresponding to the homogeneous boiling explosion (t^*, x_e) is known, the accumulated energy density in the liquid corresponding to the homogeneous boiling scale η^* (t^*, x_e) can be readily obtained from the energy density prior to the boiling explosionon the basis of the penetration depth (δ^*_{th}). By following the analytical solution of 1-D heat conduction [86], total energy through the liquid boundary prior to the boiling explosion can be obtained as:

$$E^* = \int_0^{t^*} q_w(t) dt$$

(4.16)

Now for different boundary condition, expression of boundary heat flux, $q_w(t)$, and penetration depth, δ^*_{th}, are given below:

For linearly increasing temperature boundary condition:

$$q_w(t) = \frac{2\lambda b \sqrt{t}}{\sqrt{\pi\alpha}}; \delta^*_{th} = 2.4\sqrt{4\alpha t^*}$$

(4.17a)

For constant heat flux boundary condition:

$$q_w(t) = q_w; \delta^*_{th} = 2.6\sqrt{4\alpha t^*}$$

(4.17b)

For constant temperature boundary condition:

$$q_w(t) = \frac{\lambda(T_i - T_0)}{\sqrt{\pi\alpha t}}; \delta^*_{th} = 2.7\sqrt{4\alpha t^*}$$

(4.17c)

64

4.10 Cumulative Energy Density: A Unique Criterion

For various boundary heating conditions, instantaneous non-dimensional liquid temperature, θ, instantaneous spectrum of deposited energy, distribution of relative energy density factor, m and cumulative energy density for water at initial temperature, T_0, of 20^0C have been represented against η at any instance of time in *Figs: 4.8-4.11*.

From *Figs. 4.11 and 4.12* and according to Carlslaw and Jaeger [88], the instantaneous thermal penetration depth (δ_{th}) can be approximated by η = 2.4, 2.6 and 2.7 for liquid heating with linearly increasing boundary temperature, high boundary heat flux and constant boundary temperature respectively.
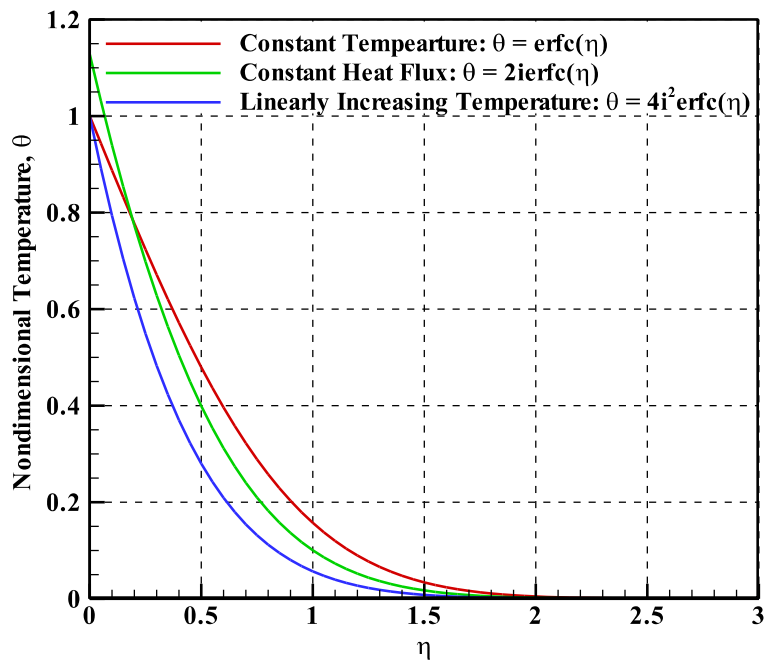
Fig. 4.11: Instantaneous spatial temperature distribution for various boundary conditions.
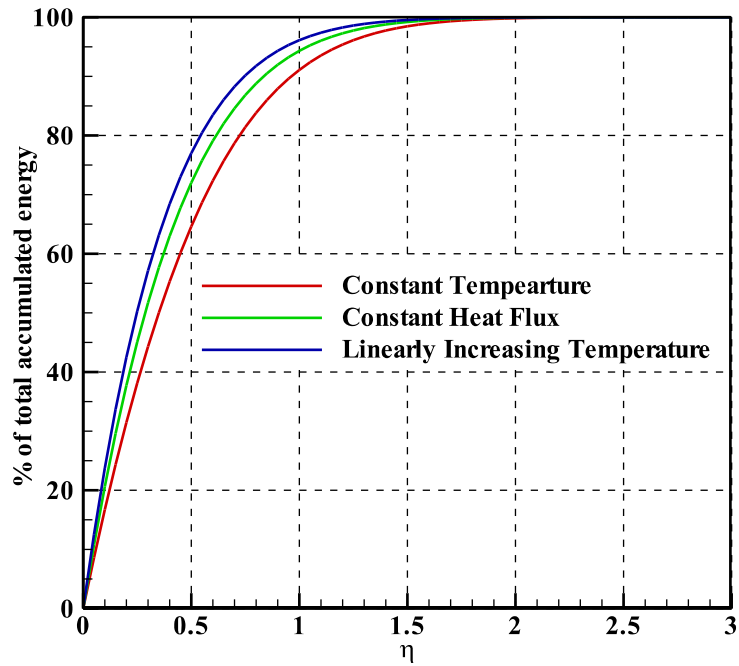
Fig. 4.12: Instantaneous spatial distribution accumulated energy for various boundary conditions.
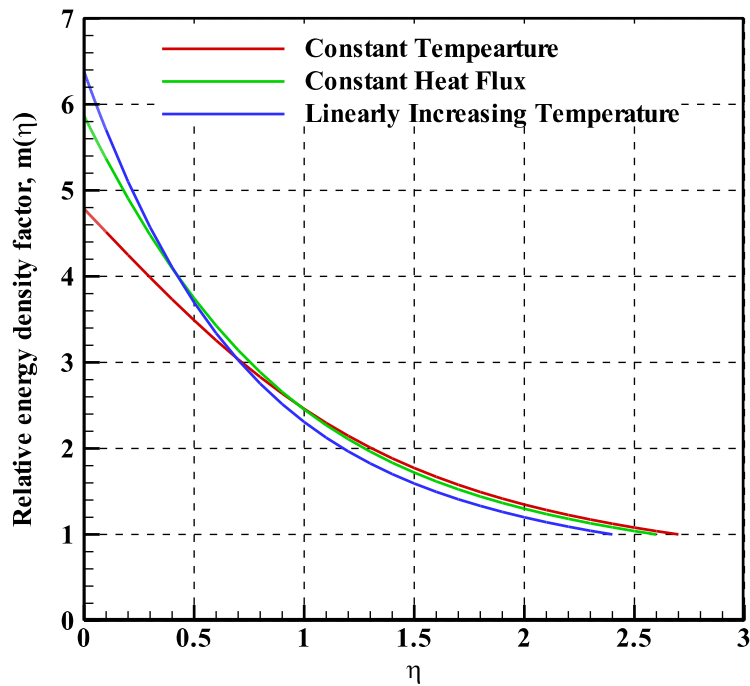
Fig. 4.13: Instantaneous spatial distribution of relative energy density factor for various boundary conditions.

66
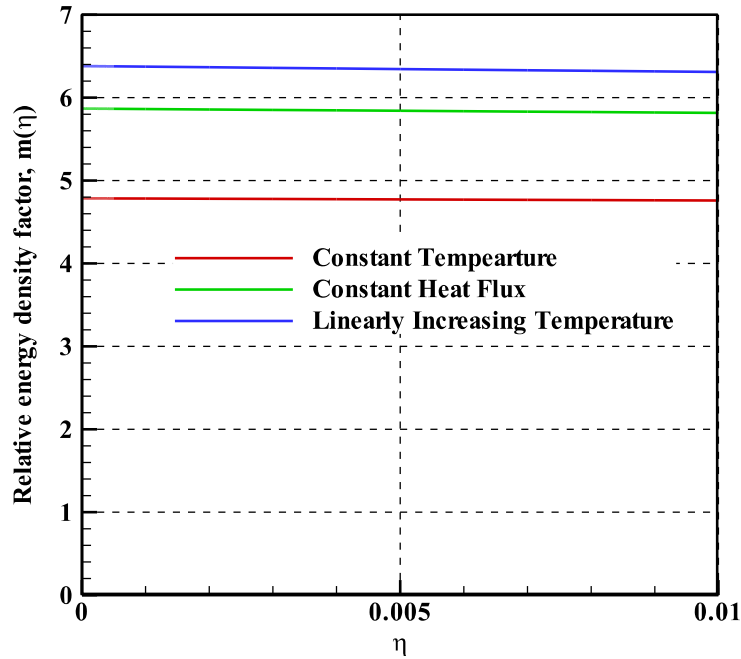
Fig. 4.14: Instantaneous spatial distribution of relative energy density factor near boundary for various boundary conditions.

Fig. 4.13 demonstrates the distribution of relative energy density factor, m with η for various liquid heating conditions. It can be noted that, for smaller values of η that essentially characterize the homogeneous boiling explosion conditions (x_e, t^*), m is several times higher than unity for any of the liquid heating cases as shown in *Fig. 4.14.*

In *Fig. 4.15 - 4.16*, for a given liquid initial condition, the cumulative energy density, $\dot{E}^*(\eta^*)$, in the liquid is plotted over a characteristic homogeneous boiling time and space scale, η^* for linearly increasing boundary condition and high heat flux boundary condition. In both figures, $\dot{E}^*(\eta^*)$ is almost constant irrespective of heating parameter and boundary condition. But with the change of liquid initial temperature, variation of $\dot{E}^*(\eta^*)$ is great. The reason behind such strong effect is that the ability of the liquid to accumulate external energy prior to homogeneous boiling depends on its initial temperature.

Fig. 4.15: Effect of liquid initial temperature on the cumulative energy density at the boiling explosion for linearly increasing boundary temperature condition.
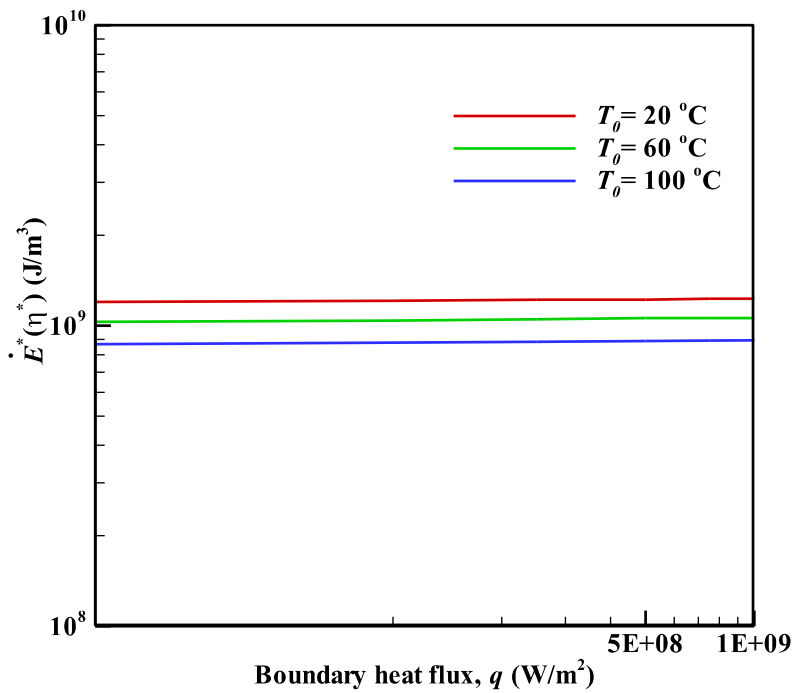
Fig. 4.16: Effect of liquid initial temperature on the cumulative energy density at the boiling explosion for high heat flux boundary condition.

The variation of the cumulative energy density, $\dot{E}^*(\eta^*)$, in the liquid over η^* and δ^*_{th} are tabulated in Tables below:

Table- 4.10: Variation of Cumulative Energy Density over a characteristic homogeneous boiling time and space scale, η^* during linear boundary heating of water (20 °C) [90]

b(K/s)	x_e(nm)	T^*_{avg}(°C)	t^*(s)	$\dot{E}^*(\delta^*_{th})$ (J/m³)	$\dot{E}^*(\eta^*)$(J/m³)
10	6.72	301.8	2.82×10^1	1.85×10^8	1.18×10^9
10^3	6.32	303.9	2.84×10^{-1}	1.86×10^8	1.19×10^9
10^5	5.88	306.3	2.87×10^{-3}	1.88×10^8	1.20×10^9
10^7	5.38	309.2	2.90×10^{-5}	1.90×10^8	1.21×10^9
10^9	4.79	312.8	2.97×10^{-7}	1.94×10^8	1.22×10^9

Table- 4.11: Variation of Cumulative Energy Density over a characteristic homogeneous boiling time and space scale, η^* during high heat flux (q) pulse heating of water (20°C) [90]

q_w(W/m²)	x_e(nm)	T^*_{avg}(°C)	t^*(s)	$\dot{E}^*(\delta^*_{th})$ (J/m³)	$\dot{E}^*(\eta^*)$(J/m³)
15×10^6	5.81	306.7	7.23×10^{-4}	2.05×10^8	1.20×10^9
100×10^6	5.39	309.1	16.547×10^{-6}	2.07×10^8	1.21×10^9
250×10^6	5.17	310.4	2.684×10^{-6}	2.08×10^8	1.22×10^9
500×10^6	5.00	311.5	6.808×10^{-7}	2.10×10^8	1.22×10^9
750×10^6	4.89	312.2	3.0601×10^{-7}	2.11×10^8	1.23×10^9
1000×10^6	4.81	312.7	1.7386×10^{-7}	2.12×10^8	1.23×10^9

Table-4.12: Variation of Cumulative Energy Density over a characteristic homogeneous boiling time and space scale, η^* during water (20 °C) contact with hot carbon steel surface ($\beta = 8.81$) [90]

T_b(°C)	T_i(°C)	x_e(nm)	T^*_{avg}(°C)	t^* (s)	$\dot{E}^*(\delta^*_{th})$ (J/m³)	$\dot{E}^*(\eta^*)$(J/m³)
336	303.9	6.41	303.4	4.4346×10^{-4}	2.48×10^8	1.18×10^9
337	304.8	6.26	304.2	1.1742×10^{-4}	2.48×10^8	1.19×10^9
338	305.7	6.12	305.0	0.3611×10^{-4}	2.49×10^8	1.19×10^9
339	306.6	5.99	305.7	0.1285×10^{-4}	2.50×10^8	1.19×10^9
340	307.5	5.87	306.3	0.5239×10^{-5}	2.51×10^8	1.20×10^9

From Table– 4.10 - 4.12, it is visible that for a certain liquid initial temperature, T_i, the cumulative energy density, $\dot{E}^*\left(\eta^*\right)$, remains in the same range regardless of boundary heating condition for water. From this observation, it can be concluded that after reaching a certain range of $\dot{E}^*\left(\eta^*\right)$ homogeneous nucleation boiling or explosive boiling of liquid will occur, regardless of boundary heating condition.

The results obtained above might be compared with that of Elias and Chambre [78] for water heating at atmospheric by uniform volumetric heating. For an initial liquid temperature of 100 °C, the cumulative energy density corresponds to a value of about 8.95×10^8 J/m^3 in the present study for water while that in the observations of Elias and Chambre [78] corresponds to about 8.46×10^8 J/m^3 for homogeneous boiling at a μs time scale. Also, $\dot{E}^*\left(\eta^*\right)$ is of same order ($\sim 10^9$ J / m^3) that is found in the study of laser ablation of water performed by Apitz and Vogel [6].
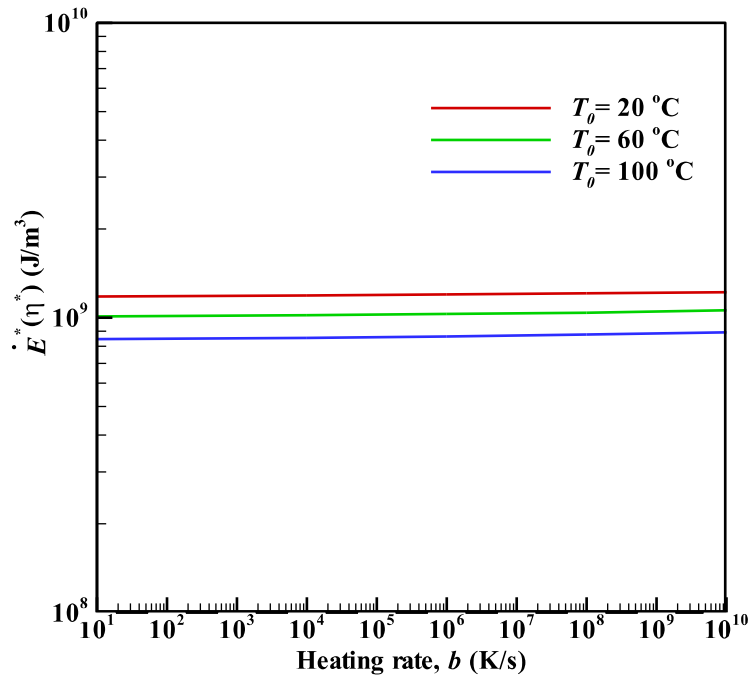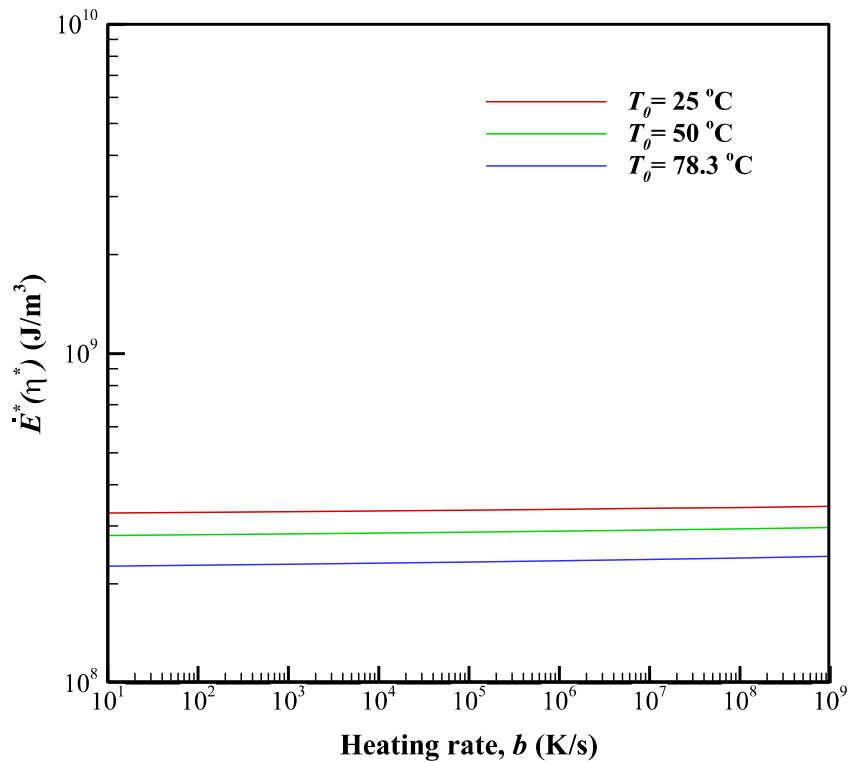

Fig. 4.17: Effect of initial temperature on the cumulative energy density at the boiling explosion for linearly increasing boundary temperature condition.

In *Fig. 4.17,* $\dot{E}^*\left(\eta^*\right)$ has been plotted against heating rate, *b*, for ethanol. From the figure, it has been observed that, the initial liquid temperature, T_0, has a strong effect on $\dot{E}^*\left(\eta^*\right)$ similar to the result found for water. The effect of initial liquid temperature, T_0, on cumulative energy density, $\dot{E}^*\left(\eta^*\right)$ is shown in tabular form below:

Table- 4.13: Variation of Cumulative Energy Density over a characteristic homogeneous boiling time and space scale, η^* during linear boundary heating of Ethanol (25°C)

b (K/s)	x_e (nm)	t^* (s)	T^*_{avg}(K)	$\dot{E}^*(\delta^*_{th})$ (J/m^3)	$\dot{E}^*\left(\eta^*\right)$(J/m^3)
10	9.11	17.165	469.65	5.14×10^7	3.28×10^8
10^3	8.57	0.1732	471.24	5.19×10^7	3.31×10^8
10^5	7.98	1.752×10^{-3}	473.08	5.25×10^7	3.35×10^8
10^6	7.65	1.763×10^{-4}	474.12	5.28×10^7	3.37×10^8
10^7	7.32	1.78×10^{-5}	475.27	5.33×10^7	3.39×10^8
10^8	6.95	1.8×10^{-6}	476.54	5.39×10^7	3.41×10^8
10^9	6.55	1.85×10^{-7}	477.97	5.55×10^7	3.44×10^8

Table- 4.14: Variation of Cumulative Energy Density over a characteristic homogeneous boiling time and space scale, η^* during linear boundary heating of Ethanol (50°C)

b (K/s)	x_e (nm)	t^* (s)	T^*_{avg}(K)	$\dot{E}^*(\delta^*_{th})$ (J/m^3)	$\dot{E}^*\left(\eta^*\right)$(J/m^3)
10	9.11	14.665	469.65	4.40×10^7	2.80×10^8
10^3	8.57	0.14826	471.24	4.44×10^7	2.84×10^8
10^5	7.98	1.5018×10^{-3}	473.08	4.50×10^7	2.87×10^8
10^6	7.65	1.5136×10^{-4}	474.12	4.54×10^7	2.89×10^8
10^7	7.32	1.5290×10^{-5}	475.27	4.58×10^7	2.91×10^8
10^8	6.95	1.553×10^{-6}	476.54	4.65×10^7	2.94×10^8
10^9	6.55	1.6005×10^{-7}	477.97	4.80×10^7	2.97×10^8

Table- 4.15: Variation of Cumulative Energy Density over a characteristic homogeneous boiling time and space scale, η^* during linear boundary heating of Ethanol (78°C)

b (K/s)	x_e (nm)	t^* (s)	T^*_{avg}(K)	$\dot{E}^*(\delta^*_{th})$ (J/m³)	$\dot{E}^*(\eta^*)$(J/m³)
10	9.11	11.834	469.65	3.55×10^7	2.26×10^8
10^3	8.57	0.11996	471.24	3.60×10^7	2.29×10^8
10^5	7.98	1.2188×10^{-3}	473.08	3.65×10^7	2.33×10^8
10^6	7.65	1.2305×10^{-4}	474.12	3.69×10^7	2.35×10^8
10^7	7.32	1.2455×10^{-5}	475.27	3.73×10^7	2.37×10^8
10^8	6.95	1.2684×10^{-6}	476.54	3.80×10^7	2.40×10^8
10^9	6.55	1.3128×10^{-7}	477.97	3.93×10^7	2.43×10^8

From Table- 4.13-4.15 and *Fig. 4.17*, it can be seen for a given T_0, $\dot{E}^*(\eta^*)$ remains in a certain range. It has already been observed for water that the range of values for $\dot{E}^*(\eta^*)$ remains almost in same order for an initial liquid temperature regardless of boundary heating. Therefore, it can be assume that this fact will remain true for ethanol. Therefore it can be stated that, for a particular initial liquid temperature, T_0, after reaching a certain range of cumulative energy density $\dot{E}^*(\eta^*)$, the explosive boiling will occur regardless of heating technique, which is the unique criterion for explosive boiling.

From *Fig. 4.16-4.17*, it is observed that, the pattern of variation of cumulative energy density $\dot{E}^*(\eta^*)$, is same for ethanol and water. But the values for water vary by an order of magnitude from the values for ethanol. From this observation, it can be stated that, value of cumulative energy density $\dot{E}^*(\eta^*)$, is dependent on the inherent molecular properties of liquid, such as, molecular attraction-repulsion forces, mass of a molecule etc.

4.11 Summary

At first, for conditions mentioned in the literature, the model predicted results were compared with the experimental observations [31] for two characteristic liquid cluster size scales. From the comparison, critical vapor embryo size scale was chosen for theoretical prediction of homogeneous boiling characteristics for ethanol heating at atmospheric pressure over a wide

range of heating. Then predicted boiling explosion conditions are clarified by the theoretical explosion condition as given by Gambill and Lienhard [80], the experimental observations noted by Avedisian [81] and satisfied the criteria of minimum time required for boiling explosion described by Lu and Ding [85]. From these observations, for the ethanol heating at atmospheric pressure, approximate equations For the time of boiling explosion, t^*(μs), and the maximum attainable liquid temperature, T^*_{avg}(K), for a wide range of boundary heating rate, b, and liquid initial temperature, T_0(K) are proposed. But in these observations, both time and temperature at the boiling explosion change with the heating parameter especially the variation of time is very drastic. To find a unique criterion for explosive boiling, cumulative energy density approach is taken. From this energy approach, it has been found that, for a particular initial liquid temperature, T_0, after reaching a certain range of cumulative energy density $\dot{E}^*\left(\eta^*\right)$, the explosive boiling will occur regardless of heating technique, for water and ethanol. So for a particular liquid, at a given initial liquid temperature, a unique criterion in the form of cumulative energy density has been found.

CHAPTER 5

CONCLUSION AND RECOMMENDATION

5.1 Conclusion

With the objective of determining the characteristics of homogeneous nucleation boiling or explosive boiling and finding unique criterion for the occurrence of the phenomenon in Ethanol under non-equilibrium heating, recently developed macroscopic model have been used in the present study. The final results of the present research are briefly stated below:

1. Macroscopic model developed by Hasan et al. [79] has been used to model the liquid heating and subsequent boiling explosion processes considering finite liquid cluster at the boundary in Ethanol.

2. The model predicted results for two different cluster size scales have been compared with experimental observations for identical conditions reported in Okuyama et al [31]. From the comparison, when critical vapor embryo size scale was chosen as the characteristic cluster size, the results are in good agreement with experimental observation. But with thermal penetration depth as characteristic cluster size, the predicted times of boiling explosion for different heating rate are almost twice the experimental observation. Also the cluster size in these two models differs roughly by 3 orders of magnitude. Therefore, critical vapor embryo size scale was chosen as the characteristic cluster size for theoretical prediction of homogeneous boiling characteristics for ethanol heating at atmospheric pressure over a wide range of non-equilibrium practical liquid heating conditions.

3. Considering critical vapor embryo at maximum cluster temperature as characteristic liquid cluster, explosive boiling conditions have been predicted for a number of heating rate $(10 - 10^9$ K/s) at a given liquid initial temperature (25^0C). It is observed from the result that the boiling explosion times vary almost in inverse order of heating rate, but the boiling explosion temperatures vary about 9^0C over the entire range of heating rate. These predictions are then validated by theoretical explosion condition proposed by Gambill and Lienhard [80] and experimental observation given by Avedisian [81]. The predicted boiling explosion times also satisfies the criteria of minimum time required for boiling explosion described by Lu and Ding [85].

4. For a wide range of boundary heating rate, b ($10 - 10^9$ K/s) and liquid initial temperature, T_0 ($25-78^0$C), the time of boiling explosion, t^*, has been determined from the model. From the obtained result, it is found that t^* is dependent on T_0 and approximate equations for the time of boiling explosion and the maximum attainable liquid temperature have been proposed for a wide range of boundary heating rate, b ($10 - 10^9$ K/s) and liquid initial temperature, T_0 ($25-78^0$C)

5. But it has been noticed in these observations that, both time and temperature at the boiling explosion change with the heating parameter especially the variation of time is very drastic. Therefore, it is concluded that, these parameters are unable to describe the unique state of explosive boiling.

6. To find the limiting condition or unique criterion, a cumulative energy density approach is taken. From this energy approach, it has been found that, for a given initial liquid temperature, the explosive boiling will occur regardless of heating technique, after reaching a certain range of cumulative energy density. From the present study, the value of cumulative energy density, $\dot{E}^*(\eta^*)$, has been found to be in the range of 1.18×10^9 - 1.23×10^9 J / m^3 for water at 20^0C and 3.28×10^8 - 3.44×10^8 J / m^3 for ethanol at 25^0C . But there is a strong variation of cumulative energy density for explosive boiling, with different liquid initial temperature. Therefore, it has been concluded that, for a given initial liquid temperature, cumulative energy density can be taken as a unique criterion or limiting condition which triggers the boiling explosion phenomenon irrespective of liquid boundary heating conditions.

5.2 Recommendation

Phase change phenomenon coupled with non-equilibrium heating is a very complex matter. Therefore, more studies are required for understanding this complex mechanism. In the present study, some assumptions are made such as the consideration of the average temperature in the liquid cluster and the application of nucleation event rate which has been derived for equilibrium condition that is for infinite liquid volume. Also the bubble growth in microscopic level is not truly spherical rather some interfacial ambiguities exist. It is to be expected that, these issues will be addressed in the future.

REFERENCES

[1] A.W. Cronenberg, Recent developments in the understanding of energetic molten fuel coolant interactions, Nucl. Safety 21 (1980) 319–337.

[2] R.C. Reid, Rapid phase transitions from liquid to vapor, Adv. Chem. Eng. 12 (1983) 105–207.

[3] P.D. Hess, K.J. Brondyke, Molten aluminum–water explosions, Met. Prog.95 (1969) 93.

[4] P.E. Schick, T.M. Grace, Review of smelt–water explosions, Project No. 3473-2, Institute of Paper Chemistry, Appleton, Wisconsin, 1982.

[5] R.C. Reid, Superheated liquids, Am. Sci. 64 (1976) 146.

[6] I.Apitz, A. Vogel, Material ejection in nanosecond Er:YAG laser ablation of water, liver and skin, Applied Physics A – Material Science & Processing, Vol. 81, pp. 329-338, 2005.

[7] http://www.wisegeek.org/what-is-nucleation.html

[8] http://wins.engr.wisc.edu/teaching/mpfBook/node27.html

[9] G. Romear-Guereca, Explosive vaporization in microenclosures and boiling phenomenon submicron thin film strip heaters, ETH, 2007

[10] http://www.imaging.org/ist/resources/tutorials/images/inkjet_printer_fig1.gif

[11] A. Asai, Application of the nucleation theory to the design of bubble jet printers, *Jpn. J. Applied Physics*, Vol. 28, pp. 909-915, 1989.

[12] Nguyen, N.-T., Wereley, S., Fundamentals and Applications of Microfluidics,2002.

[13] https://encryptedtbn1.gstatic.com/images?q=tbn:ANd9GcSP_JlLtyPDSpTD2prHSefCgA7ANP6P1M9XsDLafXwYe6Wd9oe5

[14] D. J. Laser, J. G. Santiago, A Review of Micropumps, *J. Micromech. Microeng.* Vol. 14, R35–R64, 2004.

[15] Stemme, E., Stemme, G., A valveless diffuser/nozzle-based fluid pump, Sensors and Actuators A: Physical, vol. 39 (2), pp. 159–167, 1993.

[16] Tsai, J., Lin, L., Active microfluidic mixer and gas bubble filter driven by thermal bubble micropump, Sensors and Actuators A-Physical, vol. 97 (8), pp. 665–671, 2002.

[17] Kim, J. H., Na, K. H., Kang, C. J., Kim, Y. S., A disposable thermo-pneumatic actuated Micropump stacked with PDMS layers and ITO-coated glass, Sensors andActuators A-Physical, vol. 120 (2), pp. 365–369, 2005.

[18] Yin, Z., Prosperetti, A., A microfluidic 'blinking bubble' pump, Journal of micromechanics and microengineering, vol. 15 (3), pp. 643–651, 2005.

[19] Maxwell, R., Gerhardt, A., Toner, M., Gray, M., Schmidt, M., A micro bubble powered bioparticle actuator, Journal of micro electromechanical systems, vol. 12 (5), pp. 630, 2003.

[20] Y. K. Lee, U. C. Yi, F. G. Tseng, C. J. Kim, C. M. Ho, Fuel injection by a thermal microinjector, Proceedings of MEMS, ASME International Mechanical Engineering, Nashville, Tennessee, USA, pp 419–425, 1999.

[21] Tseng, F., Shih, C., Kim, C., Ho, C., Characterization of Droplet Injector Process of a Micro-injector, US 13th National Congress of Applied Mechanics. University of Florida, 1998.

[22] D. K. Maurya, S. Das, S. K. Lahiri, Silicon MEMS vaporizing liquid microthruster with internal microheater, J. Micromech. Microeng.Vol. 15, pp. 966–970, 2005.

[23] Iyer, N., Mastrangelo, C. H., Akkaraju, S., Brophy, C., McDdonald, T. G., Dureiko, R.,Carlen, E. T., A two-dimensional optical cross-connect with integrated waveguides and surface micromachined crossbar switches. Sensors and Actuators a-Physical, vol. 109 (3), pp. 231–241, 2004.

[24] Fouquet, J., Compact Optical Cross-connect Switch Based on Total Internal Reflection in a Fluid-containing Planar Lightwave Circuit. In: Optical fiber communicating conference. Baltimore, USA, 2000.

[25] Makihara, M., Sato, M., Shimokawa, F., Nishida, Y., Micromechanical optical switches based on thermo-capillary integrated in waveguide substrate. Journal of Lightwave Technology, vol. 17 (1),pp. 14–18, 1999.

[26] V.P. Skripov, Metastable Liquids, John Wiley & Sons, New York, 1974.

[27] A. Asai, S. Hirasawa, I. Endo, Bubble generation mechanism in the bubble jet recording process, Journal of Imaging Technology, vol. 14 (5), pp. 120–124, 1988.

[28] A. Asai, Bubble dynamics in boiling under high heat flux pulse heating, Journal Heat Transfer, 113, pp. 973–979, 1991.

[29] Y. Iida, K. Okuyama, K. Sakurai, Peculiar bubble generation on a film heater submerged in ethyl alcohol and imposed a high heating rate over 10 K/s, International Journal of Heat Mass Transfer, vol. 36 (10), pp. 2699–2701, 1993.

[30] Y. Iida, K. Okuyama, K. Sakurai, Boiling nucleation on a very small film heater subjected to extremely rapid heating, International Journal of Heat Mass Transfer, vol. 37(17), pp. 2771–2780, 1994.

[31] K. Okuyama, S. Mori, K. Sawa, Y. Iida, Dynamics of boiling succeeding spontaneous nucleation on a rapidly heated small surface, International Journal of Heat Mass Transfer, vol. 49, pp. 2771–2780, 2006.

[32] Z. Zhao, S. Glod, D. Poulikakos, Pressure and power generation during explosive vaporization on a thin-film microheater, International Journal of Heat Mass Transfer, vol. 43, pp. 281–296, 2000.

[33] S. Glod, D. Poulikakos, Z. Zhao, G. Yadigaroglu, An investigation of microscale explosive vaporization of water on an ultrathin Pt wire, International Journal of Heat Mass Transfer, vol. 45, pp. 367–379, 2002.

[34] M.N. Hasan, M. Monde, Y. Mitsutake, Model for boiling explosion during rapid liquid heating, International Journal of Heat Mass Transfer, vol. 54, pp. 2844-2853, 2011.

[35] V. P. Skripov, and P. A. Pavlov, Explosive Boiling of Liquids and Fluctuation Nucleus Formation, *High Temperature (USSR)*, Vol. 8, pp. 782–787, 833–839, 1970.

[36] K. P. Derewnicki, Experimental Studies of Heat Transfer and Vapor Formation in Fast Transient Boiling, *International Journal of Heat and Mass Transfer* Vol. 28, pp. 2085–2092, 1985.

[37] A. Asai, T. Hara, and I. Endo, One Dimensional Model of Bubble Growth and Liquid Flow in Bubble Jet Printers, *Japanese Journal of Applied Physics*, Vol. 26 (10), pp. 1794–1801, 1987.

[38] A. Asai, Application of the Nucleation Theory to the Design of Bubble Jet Printer, *Japanese Journal of Applied Physics*, Vol. 28 (5), pp. 909–915, 1989.

[39] L. Lin, A. P. Pisano, and V. P. Carey, Thermal Bubble Formation on Polysilicon Micro Resistors, *ASME Journal of Heat Transfer*, Vol. 120, pp. 735–742, 1998.

[40] Y. Iida, K. Okuyama, T. Endou, and N. Kanda, Boiling Nucleation on a very small film heater subjected to extremely rapid heating (Effect of Ambient Pressure on Bubble Formation by Fluctuation Nucleation), JSME International Journal Series B, Vol. 40 (2), pp. 250–256, 1997.

[41] K. Okuyama, and Y. Iida, Boiling Bubble Behavior and Heat Transfer Succeeding Spontaneous Nucleation on a Film Heater, in Proceedings of 11th International Heat Transfer Conference, Vol. 2, pp. 527–532, 1998.

[42] C. T. Avedisian, W. S. Osborne, F. D. McLeod, and C. M. Curly, Measuring Bubble Nucleation Temperature on the Surface of a Rapidly Heated Thermal Ink-Jet Heater Immersed in a Pool of Water, Proceedings of Royal Society, London, A 445, pp. 3875–3899.

[43] G. Romera-Guerca, T.Y. Choi, and D. Poulikakos, Explosive vaporization and micro bubble oscillations on submicron width thin film strip heater, *International Journal of Heat and Mass Transfer*, Vol. 51, pp. 4427–4438, 2008.

[44] Z. Yin, A. Prosperetti, and J. Kim, Bubble Growth on an Impulsively Powered Microheater, *International Journal Heat and Mass Transfer*, Vol. 47, pp. 1053–1067, 2004.

[45] J. Y. Jung, J. Y. Lee, H. C. Park and H. Y. Kwak, Bubble Nucleation on Micro Line Heaters under Steady or Finite Pulse of Voltage Input, *International Journal Heat and Mass Transfer*, Vol. 46, pp. 3897–3907, 2003.

[46] P. G. Deng, Y. K. Lee, and P. Cheng, An Experimental Study of Heater Size Effect on Micro Bubble Generation, *International Journal Heat and Mass Transfer*, Vol. 49, pp. 2535–2544, 2006.

[47] V. V. Kuznetsov, and I. A. Kozulin, Explosive Vaporization of a Water Layer on a flat Microheater, *Journal of Engineering Thermophysics*, Vol. 19 (2), pp. 102–109, 2010.

[48] J. Xu, and W. Zhang, Effect of Pulse Heating Parameters on the Microscale Bubble Dynamics at a Microheater Surface, *International Journal Heat and Mass Transfer*, Vol. 51, pp. 389–396, 2008.

[49]   Yu. D. Varlamov, Yu. P. Meshcheryakov, M. P. Predtechenskii, S. I. Lezhnin and S. N. Ulýankin, Specific Features of Explosive Boiling of Liquids on a Film Microheater, *Journal of applied Mechanics and technical physics*, Vol. 48 (2), pp. 213–220, 2007.

[50]   Y. Hong, N. Ashgriz, and J, Andrews, Experimental Study of Bubble Dynamics on a Micro Heater Induced by Pulse Heating, *ASME Journal of Heat Transfer*, Vol. 126, pp. 259–271, 2004.

[51]   C. Rembe, S. aus der Wiesche, and E. P. Hofer, Thermal Ink Jet Dynamics: Modeling, Simulation and Testing, *Microelectronics Reliability*, Vol. 40, pp. 525–532, 2000.

[52]   P. Chen, W. Chen, and S. H. Chang, Bubble Growth and Ink Ejection Process of a thermal Ink Jet Print Head, *International Journal of Mechanical Science*, Vol. 39 (6), pp. 683–695, 1997.

[53]   J. R. Andrews, and M. P. O'horo, High Speed Stroboscopic System for Visualization of Thermal Ink Jet Processes, In J. Bares (Ed.), Proceedings of Photo-Optical Instrumentation Engineers (SPIE), Vol. 2413, pp. 176–181, 1995.

[54]   V. P. Carey, and A. P. Wemhoff, Thermodynamic Analysis of near Wall Effects on Phase Stability and Homogeneous Nucleation during Rapid Surface Heating, *International Journal Heat and Mass Transfer*, Vol. 48, pp. 5431–5445, 2005.

[55]   V. Gerweck and G. Yadigaroglu, A local Equation of State for Fluid in the Presence of a wall and Its Application to Rewetting, *International Journal Heat and Mass Transfer*, Vol. 35, pp. 1823–1832, 1992.

[56]   I. Ueno and M. Shoji, Thermal-Fluid Phenomena Induced by Nanosecond-Pulse Heating of Materials in Water, *ASME Journal of Heat Transfer*, Vol. 123, pp. 1123–1133, 2001.

[57]   X. Huai, Z. Dong, D. Liu, and G. Wang, An Experimental Study of Microscopic Explosive Boiling Induced by Pulsed-Laser Irradiation, Proceedings of ASME International Mechanical Engineering Congress, Vol. 3, pp. 205–212, 2002.

[58]   X. Huai, Z. Dong, D. Liu, Z. Dong, R. Jin, and G. Wang, Rapid Transient Explosive Boiling of binary Mixture under Pulsed-Laser Irradiation, *Science in China (Series E)*, Vol. 46 (5), pp. 490–496, 2003.

[59]   Yu. E. Geints, A. A. Zemlyanov, and R. L. Armstrong, Explosive Boiling of water droplets irradiated with intense Co_2-laser radiation: Numerical Experiments, *Applied Optics*, Vol. 33 (24), pp. 5805–5810, 1994.

[60]   R. D. Henry, and H. K. Fauske, Nucleation Process in Large Scale Vapor Explosions, *ASME Journal of Heat Transfer*, Vol. 101, pp. 280–287, 1979.

[61]   A. Inoue, and S. G. Bankoff, Destabilization of Film Boiling due to Arrival of Pressure Shock, Part I Experimental, *ASME Journal of Heat Transfer*, Vol. 103, pp. 459–464, 1981.

[62]   A. Inoue, A. Ganguli, and S. G. Bankoff, Destabilization of Film Boiling due to Arrival of Pressure Shock, Part II Experimental, *ASME Journal of Heat Transfer*, Vol. 103, pp. 465–471, 1981.

[63] M. Ochiai, and S. G. Bankoff, A Local Propagation Theory for Vapor Explosion, Paper No. SNI 6/3, in the Proceedings of Third Special Meeting on Sodium/Fuel Interactions in Fast Reactors, Tokyo, Japan, 1976.

[64] Y. Iida, T. Takashima, T. Watanabe, H. Ohura, C. Ogiso and N. Araki, A Fundamental Study of Thermal Interaction of Molten Salt and Cold Liquid, in the Proceedings of 19th National Heat Transfer Symposium of Japan, Nagoya, pp. 511–513, 1982.

[65] P. Spiegler, J. Hopenfeld. M. Silberberg, C. F. Bumpus Jr., and A. Norman, Onset of Stable Film Boiling and the Foam Limit, *International Journal of Heat and Mass Transfer* Vol. 6, pp. 987–994, 1963.

[66] F. S. Gunnerson, and A. W. Cronenberg, A Thermodynamic Prediction of the Temperature for Film Boiling Destabilization and its Relation to Vapor Explosion Phenomena, ANS Annual meeting, Sandiego, USA, 1978.

[67] N. Zhang, and W. J. Yang, Evaporation and Explosion of Liquid Drops on a Heated Surface, *Experiments in Fluids*, Vol. 1, pp. 101–111, 1983.

[68] S. Inada, and W. J. Yang, Mechanism of Miniaturization of Sessile Drops on a Heated Surface, *International Journal Heat and Mass Transfer*, Vol. 36, pp. 1505–1515, 1993.

[69] J. G. Eberhart, The Thermodynamic and the Kinetic Limits of Superheat of a Liquid, Journal of Colloid and Interface Science,Vol. 56(2) pp. 262–269, 1976.

[70] J. H. Lienhard, Corresponding States Correlations of the Spinodal and Homogeneous Nucleation Limits, *Journal of Heat Transfer*,Vol. 104, pp. 379–381, 1984.

[71] M. Volmer, and A. Webber, Keimbildung in ubersattigtenGebilden, *Z. Phys. Chem.*, Vol. 119, pp. 277–301, 1926.

[72] W. Doring, Die Uberhitzungsgrenzeund ZerreibfestigkeitvonFlussigkeiten, *Z. Phys. Chem.*, Vol. 36, pp. 371–386, 1937.

[73] M. Blander, and J. L. Katz, Bubble Nucleation in Liquids, *AIChE Journal*, Vol. 21(5), pp. 833–848, 1975.

[74] V. P. Carey, Liquid-Vapor Phase Change Phenomena, Hemisphere Publishing Corporation, 1994

[75] R. Cole, Boiling Nucleation, Advances in Heat Transfer, Academic Press, Vol. 10, pp. 86–166, 1974.

[76] H. Li, E. Elias, A. S. Mujumdar, Theoretical Simulation of Explosive Boiling, *International Communications in Heat and Mass Transfer*, Vol. 32, pp. 612–619, 2005.

[77] E. Elias, and M. Shusser, Lifetime of a Superheated Liquid, *Heat Mass Transfer*, Vol. 42 pp. 51–55, 2005.

[78] E. Elias, P. L. Chambre, Liquid Superheat during Non equilibrium Boiling, *Heat Mass Transfer*, Vol. 45, pp. 659–662, 2009.

[79] M. N. Hasan, M. Monde, and Y. Mitsutake, Model for Boiling Explosion during Rapid Liquid Heating, *International Journal Heat and Mass Transfer*, Vol. 54, pp. 2844–2853, 2011.

[80] W. R. Gambill, J. H. Lienhard, An upper bound for the critical boiling heat flux, ASME Journal of Heat Transfer, Vol. 111, pp. 815–818, 1989.

[81] C. T. Avedisian, The Homogeneous Nucleation Limit of Liquid, Journal of Physics and Chemistry Reference Data, Vol. 14, No. 3, Page-695-729, 1985

[82] N. I. Kolev, Multiphase Flow Dynamics, 3rd Edition, Vol. 2, Springer, Berlin, 2007.

[83] M. Gad-el-Hak, The Fluid Mechanics of Microdevices-the Freeman Scholar Lecture, *Journal of Fluid Engineering*, Vol. 121, pp690–700, 1999.

[84] M. N. Hasan, M. Monde, Review of Homogeneous Nucleation Boiling phenomena under non-equilibrium heating condition and a generalized model for boiling explosion, *Trend inJournal Heat and Mass Transfer*, Vol. 13, 2013.

[85] J.F. Lu, J. Ding, Microscopic activation near the wall during explosive boiling, *International Journal of Heat and Mass Transfer*, Vol. 47, pp. 857-862, 2011.

[86] M. N. Hasan, M. Monde, and Y. Mitsutake, Homogeneous Boiling Explosion during High Heat Flux Pulse Heating of Water, Article in press, *Journal of Thermal Science and Engineering*, Heat Transfer Society, Japan.

[87] M. N. Hasan, M. Monde, and Y. Mitsutake, Lower Limit of Homogeneous Nucleation Boiling Explosion for Water, *International Journal Heat and Mass Transfer*, Vol. 54, pp. 3226–3233, 2011.

[88] H. S. Carslaw, J. C. Jaeger, Conduction of heat in Solids, 2ndEdition, Oxford University Press, New York 1959.

[89] PROPATH Group, PROPATH: A Program Package for Thermophysical Properties, version 13.1, July, 2008.

[90] M. N. Hasan, A. Hasan, S. Ilias, Y. Mitsutake, M. Monde, Homogeneous Boiling Explosion Condition: From an Energy Point of View, Procedia Engineering, Vol. 90, pp. 618-623, 2014